

**NASA TECHNICAL  
MEMORANDUM**

**NASA TM X-72635**  
COPY NO.

NASA TM X-72635

**AERODYNAMIC DAMPING AND OSCILLATORY STABILITY IN PITCH  
AND YAW OF A MODEL OF A PROPOSED MANNED  
LIFTING ENTRY VEHICLE AT MACH NUMBERS  
FROM 0.20 TO 1.20**

By Robert A. Kilgore and Edwin E. Davenport

January 2, 1975

(NASA-TM-X-72635) - AERODYNAMIC DAMPING AND  
OSCILLATORY STABILITY IN PITCH AND YAW OF A  
MODEL OF A PROPOSED MANNED LIFTING ENTRY  
VEHICLE AT MACH NUMBERS FROM 0.20 TO 1.20  
(NASA) 40 p HC \$3.75

N75-16512

Unclas  
10222

CSCL 01C G3/02

This informal documentation medium is used to provide accelerated or special release of technical information to selected users. The contents may not meet NASA formal editing and publication standards, may be revised, or may be incorporated in another publication.

**NATIONAL AERONAUTICS AND SPACE ADMINISTRATION  
LANGLEY RESEARCH CENTER, HAMPTON, VIRGINIA 23665**

LANGLEY RESEARCH CENTER HIGH-NUMBER TM X DOCUMENT  
APPROVAL, CONTROL, AND DISTRIBUTION RECORD

Document Description

NASA TM X-72635 Dated 1/21/75 Title Aerodynamic Damping and Oscillatory Stability  
in Pitch and Yaw of a Model of a Proposed Manned Lifting Entry Vehicle at Mach Numbers  
From 0.20 to 1.20  
Author(s) Robert A. Kilgore and Edwin E. Davenport  
Section Veh.-Dyns. Branch FDB Div/Proj STAD Directorate Aeronautics  
RTR JO P3852 Test Facility/Vehicle 8-Foot TPT/SV-5P  
Sponsor Project

Dissemination Restrictions

(Fill all blanks, i.e., U,C,S, -RD,GDS,Exempt,Date,Yes,No,Country,Name, or NA)

Security Class: Document U Title U Abstract U Downgrade NA  
Declassify Dec. 31 NA; Proprietary Info. NA; Copyrighted NA; Sponsor/  
Owner Approval Req'd on Distribution NA; Pat. Off. Security Notice NA  
Foreign Exclusion NA; Immed. Foreign Limited to NA  
Authority of NA; FEED NA Foreign Release Date NA  
Authority of NA  
STIF Release for: Data Base Yes Announce and Distribute Yes  
NTIS Distribution Yes  
STIF/NTIS Delayed Announce and Distribute Date NA  
Other Limitations NA

Future Reporting Plan for Material in This Document

(Check Appropriate Box and Fill in Any Associated Lines)

- This is an interim release of an editorial copy of a formal publication.  
 Interim release to be converted to a formal publication by (date) \_\_\_\_\_  
 Interim release of material to be combined with additional material  
and converted to a formal publication by (date) \_\_\_\_\_  
 Collateral release of a paper for (publication in) (presentation at) the  
not to be announced or distributed before (date) \_\_\_\_\_  
 This is the final release of special information not suitable for formal  
publication which serves the following need: Contribution to the aerodynamic  
data base for future studies of lifting-body vehicles.  
 Other: \_\_\_\_\_  
\*Necessity for interim accelerated release: \_\_\_\_\_

Checking, Approvals, and Distribution

Document, Reporting Plan, Restrictions, and Distribution Approved by:  
Author(s) Robert A. Kilgore Edwin E. Davenport Date 15 Jan 1975  
Section Head Date Branch Head E.C. Polham Date 1-24-75  
Div. Ch./Proj. Mgr. R.E.H. Date 1/21/75 Dir. Reis Date 1-21-75  
\*Classification and Limited Access Authorized by Date  
\*Recipient Clearance and Handling Checked by Date  
Patent Office release approval by Wallace Nelson Date 2-3-75  
Report and Manuscript Control Office, M/S 180A Date  
Publications Branch, M/S 180 Date

\* If Classified

Initial Distribution List

(Check Appropriate Box, Fill in Lines, and/or Add Distribution List)

Number of Copies Prepared 100 "A" List Distributed (date) 2-26-75

- Space Shuttle Information Distribution by JSC Data Man Procedures  
 Standard Distribution List for \_\_\_\_\_

Distribution Specified Below:

A. Basic Distribution to be Made Directly by LaRC Publications Branch:

<u>Copies</u>	<u>Copy Nos.</u>	<u>Addresses</u>	<u>Special Notes</u>
*1		LaRC Central Files - With signed original of this form	
0		LaRC Report & Manuscript - Copy of this form only	
		Control Office	
6		LaRC Library	
1		LaRC Technology Utilization Office	
2		Lewis Library	
2		Ames Library	
2		FRC Library	
2		JSC Library	
2		MSFC Library	
2		KSC Library	
2		JPL Library	
2		Goddard Library	
2		NASA Headquarters Library	
30		NASA STIF Attn: Input Section - With copy of this form	

\*Route through Report and Manuscript Control Office (M/S 180A)

B. Supplementary distribution to be made by originating organization:  
(The Langley Central Files must be notified of subsequent changes in distribution by a copy of transmittal letters or appropriate memorandums)

<u>Copies</u>	<u>*Copy Nos.</u>	<u>Addresses</u>	<u>Special Notes</u>
25		Author (s) Robert A. Kilgore Edwin E. Davenport	
1		Veh.-Dyng. Section	
1		FDB Branch	
1		STAD Div/Proj.Off.	

1. Report No. NASA TM X-72635		2. Government Accession No.		3. Recipient's Catalog No.	
4. Title and Subtitle Aerodynamic Damping and Oscillatory Stability in Pitch and Yaw of a Model of a Proposed Manned Lifting Entry Vehicle at Mach Numbers From 0.20 to 1.20				5. Report Date January 2, 1975	
				6. Performing Organization Code	
7. Author(s) Robert A. Kilgore and Edwin E. Davenport				8. Performing Organization Report No.	
9. Performing Organization Name and Address NASA Langley Research Center Hampton, Virginia 23665				10. Work Unit No.	
				11. Contract or Grant No.	
12. Sponsoring Agency Name and Address National Aeronautics and Space Administration Washington, D. C. 20546				13. Type of Report and Period Covered High-Number TM X	
				14. Sponsoring Agency Code	
15. Supplementary Notes Special technical information release, not planned for formal NASA publication.					
16. Abstract  Wind-tunnel tests have been made at angles of attack from about $-2^{\circ}$ to about $22^{\circ}$ at $0^{\circ}$ angle of sideslip by using a small-amplitude forced-oscillation technique. Models were tested with upper and lower control flaps both deflected and undeflected. The configuration with flaps deflected has positive damping in both pitch and yaw and is stable in both pitch and yaw except at the higher angles of attack where the tail surfaces are submerged in the wake from the body.					
17. Key Words (Suggested by Author(s)) (STAR category underlined) Lifting entry vehicle, <u>Aerodynamics</u> Dynamic stability, Transonic				18. Distribution Statement  Unclassified-Unlimited	
19. Security Classif. (of this report) Unclassified		20. Security Classif. (of this page) Unclassified		21. No. of Pages 39	22. Price* \$3.75

\*Available from { The National Technical Information Service, Springfield, Virginia 22151  
{ STIF/NASA Scientific and Technical Information Facility, P.O. Box 33, College Park, MD 20740

NATIONAL AERONAUTICS AND SPACE ADMINISTRATION

AERODYNAMIC DAMPING AND OSCILLATORY STABILITY IN PITCH  
AND YAW OF A MODEL OF A PROPOSED MANNED  
LIFTING ENTRY VEHICLE AT MACH NUMBERS  
FROM 0.20 TO 1.20

By Robert A. Kilgore and Edwin E. Davenport

ABSTRACT

Wind-tunnel tests have been made at angles of attack from about  $-2^{\circ}$  to about  $22^{\circ}$  at  $0^{\circ}$  angle of sideslip by using a small-amplitude forced-oscillation technique. Models were tested with upper and lower control flaps both deflected and undeflected. The configuration with flaps deflected has positive damping in both pitch and yaw and is stable in both pitch and yaw except at the higher angles of attack where the tail surfaces are submerged in the wake from the body.

NATIONAL AERONAUTICS AND SPACE ADMINISTRATION

AERODYNAMIC DAMPING AND OSCILLATORY STABILITY IN PITCH  
AND YAW OF A MODEL OF A PROPOSED MANNED  
LIFTING ENTRY VEHICLE AT MACH NUMBERS  
FROM 0.20 TO 1.20

By Robert A. Kilgore and Edwin E. Davenport

SUMMARY

Wind-tunnel measurements of the aerodynamic damping and oscillatory stability in pitch and yaw of a sub-scale model of a proposed manned lifting entry vehicle have been made by using a small-amplitude forced-oscillation technique. The investigation was made at Mach numbers from 0.20 to 1.20 at angles of attack from about  $-2^\circ$  to about  $22^\circ$  at  $0^\circ$  angle of sideslip. Models were tested with upper and lower control flaps both deflected and undeflected.

With undeflected flaps, the damping in pitch is generally near zero or slightly positive and, except at the lower Mach numbers, is nonlinear with angle of attack. With deflected flaps the level of damping is generally increased and results in positive damping in pitch at all test conditions. With undeflected flaps, the model exhibits negative stability in pitch except at the lower Mach numbers. In general, with flaps deflected the model has positive stability throughout the angle of attack range except for the higher angles of attack.

Both configurations have positive damping in yaw which generally increases with increasing angle of attack. Both configurations generally exhibit a decrease in stability in yaw with angle of attack. The configuration with flaps deflected has positive stability for angles of attack less than about  $12^\circ$ . However, except at the lower Mach numbers the configuration with flaps undeflected is unstable over a large range of angle of attack.

## INTRODUCTION

In order to design adequate guidance and control systems for any of the proposed manned lifting entry vehicles, it was necessary to know both the static and dynamic stability characteristics of the vehicle for all flight conditions. Therefore, as a part of the NASA support of the program to develop a manned lifting entry vehicle, wind-tunnel tests were made at the Langley Research Center to determine some of the dynamic-stability characteristics of a proposed lifting entry vehicle. Data obtained in pitch for the proposed vehicle at Mach numbers of 1.80, 2.16, and 2.86 are reported in reference 1. The tests reported herein were made in both pitch and yaw at Mach numbers from 0.20 to 1.20. The tests were made at angles of attack from about  $-2^\circ$  to about  $22^\circ$  at  $0^\circ$  angle of sideslip by using a small-amplitude forced-oscillation technique. The results of these tests, obtained in the Langley 8-foot transonic pressure tunnel during 1965, were used during the lifting entry design studies. The results are published herein to provide a contribution to the aerodynamic data base for future studies of lifting body vehicles.

## SYMBOLS

Measurement and calculations were made and are given in the International System of Units (SI). Details concerning the use of SI, together with physical constants and conversion factors, are given in reference 2.

The aerodynamic parameters are referred to the body system of axes as shown in figure 1, in which the coefficients, angles, and angular velocities are shown in the positive sense. These axes originate at the center of oscillation of the model, as shown in figure 2. The equations used to reduce the data are presented in the section on "Procedure and Reduction of Data".

A	reference area, 0.0963 m <sup>2</sup>
C <sub>m</sub>	pitching moment coefficient, $\frac{\text{Pitching moment}}{q_{\infty}Ad}$ , (see fig. 1)
C <sub>m<sub>q</sub></sub>	$\frac{\partial C_m}{\partial \left(\frac{qd}{2V}\right)}$ per radian
C <sub>m<sub>q</sub><sup>2</sup></sub>	$\frac{\partial C_m}{\partial \left(\frac{qd^2}{4V^2}\right)}$ per radian
C <sub>m<sub>α</sub></sub>	$\frac{\partial C_m}{\partial \alpha}$ per radian
C <sub>m<sub>α̇</sub></sub>	$\frac{\partial C_m}{\partial \left(\frac{\dot{\alpha}d}{2V}\right)}$ per radian
C <sub>m<sub>q</sub></sub> + C <sub>m<sub>α̇</sub></sub>	damping-in-pitch parameter, per radian
C <sub>m<sub>α</sub></sub> - k <sup>2</sup> C <sub>m<sub>q</sub></sub>	oscillatory-longitudinal-stability parameter, per radian
C <sub>n</sub>	yawing-moment coefficient, $\frac{\text{Yawing moment}}{q_{\infty}Ad}$ , (see fig. 1)
C <sub>n<sub>r</sub></sub>	$\frac{\partial C_n}{\partial \left(\frac{rd}{2V}\right)}$ per radian
C <sub>n<sub>r</sub><sup>2</sup></sub>	$\frac{\partial C_n}{\partial \left(\frac{rd^2}{4V^2}\right)}$ per radian
C <sub>n<sub>β</sub></sub>	$\frac{\partial C_n}{\partial \beta}$ per radian
C <sub>n<sub>β̇</sub></sub>	$\frac{\partial C_n}{\partial \left(\frac{\dot{\beta}d}{2V}\right)}$ per radian
C <sub>n<sub>r</sub></sub> - C <sub>n<sub>β̇</sub></sub> cos α	damping-in-yaw parameter, per radian

$C_{n\beta} \cos \alpha + k^2 C_{nr}$	oscillatory-directional-stability parameter, per radian
d	reference length, 0.5608 m for pitch tests, 0.2438m for yaw tests
f	frequency of oscillation, hertz
k	reduced-frequency parameter, $\frac{\omega d}{2V}$ , radians
M	free-stream Mach number
q	angular velocity of model about Y-axis, radians/second (see fig. 1)
$q_\infty$	free-stream dynamic pressure, $N/m^2$
R	Reynolds number based on 0.5608 m
r	angular velocity of model about Z-axis, radians/second (see fig. 1)
V	free-stream velocity, m/s
X,Y,Z	body system of axes (see fig. 1)
$\alpha$	angle of attack, degrees or radians or mean angle of attack, degrees (see fig. 1)
$\beta$	angle of sideslip, radians (see fig. 1)
$\omega$	angular velocity, $2\pi f$ , radians/second

A dot over a quantity denotes the first derivative with respect to time.

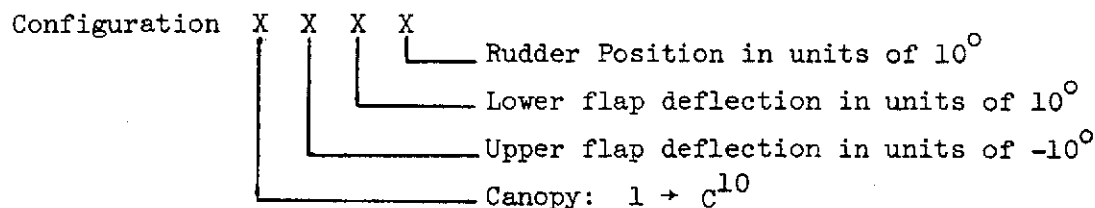
The expression  $\cos \alpha$  appears in the damping-in-yaw and oscillatory-directional-stability parameters because these parameters are expressed in the body system of axes.

## APPARATUS

### Models

Design dimensions of the sub-scale models of the configurations tested are presented in the sketches of figure 2. Details of the geometric characteristics of the models are given in table I. The models were geometrically similar to the proposed configurations except for the aft portions which were modified to provide clearance for the model-support sting. A single body portion, made of fiberglass reinforced plastic, was used for both configurations. The upper and lower flaps were made of aluminum alloy and were bolted to the model. With the flaps removed, the fiberglass reinforced plastic portion of the model represented the  $0^\circ$  flap deflection configuration. The fiberglass reinforced plastic rudders were fixed in the  $0^\circ$  position. The canopy was made of mahogany. The surfaces of the models exposed to the airstream were aerodynamically smooth.

A four digit code is used to identify the configurations. The configuration code as well as the designation of the various model components were assigned by the prime contractor for the proposed vehicle for identification of the various configurations tested. The configuration code is as follows:



Thus, the code 1320 represents the model with the  $C^{10}$  canopy, upper flaps set at  $-30^\circ$ , lower flaps set at  $20^\circ$ , and rudder set at  $0^\circ$ . Photographs of configuration 1320 mounted on the oscillation-balance mechanism are presented as figure 3.

## Oscillation-Balance Mechanism

A view of the forward portion of the oscillation-balance mechanism which was used for these tests is presented in figure 4. Since the oscillation amplitude is small ( $\sim 1^\circ$ ), the rotary motion of a variable-speed electric motor is used to provide essentially sinusoidal motion of nearly constant amplitude to the balance through the crank and crosshead mechanism. The oscillatory motion is about the pivot axis which was located at the model station corresponding to the proposed center of mass of the full-scale configuration.

The strain-gage bridge which measures the torque required to oscillate the model is located between the model attachment surface and the pivot axis. This torque-bridge location eliminates the effects of pivot friction and the necessity to correct the data for the changing pivot friction associated with changing aerodynamic loads. Although the torque bridge is physically forward of the pivot axis, the electrical center of the bridge is located at the pivot axis so that all torques are measured with respect to the pivot axis.

A mechanical spring, which is an integral part of the fixed balance support, is connected to the oscillation balance at the point of model attachment by means of a flexure plate. The mechanical spring and flexure plate were electron-beam welded in place after assembly of the oscillation-balance support in order to minimize mechanical friction. A strain-gage bridge, fastened to the mechanical spring, provides a signal proportional to the model angular displacement with respect to the sting.

## Wind Tunnel

The tests reported herein were made in the Langley 8-foot transonic pressure

tunnel. The test section of this single-return tunnel is about 2.2 meters square with slotted upper and lower walls to permit continuous operation through the transonic-speed range. Mach numbers from near 0 to 1.30 can be obtained and kept constant by controlling the speed of the tunnel-fan drive motor. Relative humidity and total temperature of the air can be controlled in order to minimize the effects of condensation shocks. Total pressure can be varied in order to obtain the desired test Reynolds number. The sting-support strut is designed to keep the model near the centerline of the tunnel through a range of angle of attack from about  $-2^{\circ}$  to  $22^{\circ}$  when used with the oscillation-balance mechanism which was used for these tests. A more detailed description of the Langley 8-foot transonic pressure tunnel is given in reference 3.

#### PROCEDURE AND REDUCTION OF DATA

For the pitching tests, measurements are made of the amplitude of the torque required to oscillate the model in pitch  $T_Y$ , the amplitude of the angular displacement in pitch of the model with respect to the sting  $\Theta$ , the phase angle  $\eta$  between  $T_Y$  and  $\Theta$ , and the angular velocity of the forced oscillation  $\omega$ . Some details of the electronic instrumentation used to make these measurements are given in reference 4. The viscous-damping coefficient in pitch  $C_Y$  for this single-degree-of-freedom system is computed as

$$C_Y = \frac{T_Y \sin \eta}{\omega \Theta}$$

and the spring-inertia parameter in pitch is computed as

$$K_Y - I_Y \omega^2 = \frac{T_Y \cos \eta}{\Theta}$$

where  $K_Y$  is the torsional-spring coefficient of the system and  $I_Y$  is the moment of inertia of the system about the body Y-axis.

The damping-in-pitch parameter was computed as

$$C_{m_q} + C_{m_{\dot{\alpha}}} = - \frac{2V}{q_{\infty} Ad^2} \left[ (C_Y)_{\text{wind on}} - (C_Y)_{\text{wind off}} \right]$$

and the oscillatory-longitudinal-stability parameter was computed as

$$C_{m_{\alpha}} - k^2 C_{m_{\dot{q}}} = - \frac{1}{q_{\infty} Ad} \left[ (K_Y - I_Y \omega^2)_{\text{wind on}} - (K_Y - I_Y \omega^2)_{\text{wind off}} \right]$$

Since the wind-off value of  $C_Y$  is not a function of oscillation frequency, it is determined at the frequency of wind-off velocity resonance because  $C_Y$  can be determined most accurately at this frequency. The wind-off value of  $K_Y - I_Y \omega^2$  is determined at the same frequency as the wind-on value of  $K_Y - I_Y \omega^2$  since this parameter is a function of frequency.

For the yawing tests, measurements are made of the amplitude of the torque required to oscillate the model in yaw  $T_Z$ , the amplitude of the angular displacement in yaw of the model with respect to the sting,  $\Psi$ , the phase angle  $\lambda$  between  $T_Z$  and  $\Psi$ , and the angular velocity of the forced oscillation  $\omega$ . The viscous-damping coefficient in yaw for this single-degree-of-freedom system is computed as

$$C_Z = \frac{T_Z \sin \lambda}{\omega \Psi}$$

and the spring-inertia parameter in yaw is computed as

$$K_Z - I_Z \omega^2 = \frac{T_Z \cos \lambda}{\Psi}$$

where  $K_Z$  is the torsional-spring coefficient of the system and  $I_Z$  is the moment of inertia of the system about the body Z-axis.

For these tests, the damping-in-yaw parameter was computed as

$$C_{n_r} - C_{n_{\dot{\beta}}} \cos \alpha = - \frac{2V}{q_{\infty} A d^2} \left[ (C_Z)_{\text{wind on}} - (C_Z)_{\text{wind off}} \right]$$

and the oscillatory-directional-stability parameter was computed as

$$C_{n_{\beta}} \cos \alpha + k^2 C_{n_r} = \frac{1}{q_{\infty} A d} \left[ (K_Z - I_Z \omega^2)_{\text{wind on}} - (K_Z - I_Z \omega^2)_{\text{wind off}} \right]$$

The wind-off value of  $C_Z$  is determined at the frequency of wind-off velocity resonance and the wind-off and wind-on values of  $K_Z - I_Z \omega^2$  are determined at the same frequency.

#### TEST CONDITIONS

The tests were made at selected Mach numbers from 0.20 to 1.20 at angles of attack from  $-2^\circ$  to about  $22^\circ$  at  $0^\circ$  angle of sideslip. Reynolds number, based on a reference length of 0.5608 meters, stagnation pressure, and stagnation temperature for the various Mach numbers were as follows:

Mach number, M	Stagnation pressure, N/m <sup>2</sup>	Stagnation temperature, K	Reynolds number, R
1.20	45.2 x 10 <sup>3</sup>	323	3.46 x 10 <sup>6</sup>
1.00	46.0	322	3.43
.95	47.2	322	3.47
.90	48.4	322	3.49
.80	50.5	322	3.46
.60	60.3	321	3.48
.40	80.0	319	3.38
.20	149.6	317	3.35

The data were obtained at an oscillation amplitude of about  $1^\circ$  (one half of peak to peak) with the model-balance system oscillating at or near the frequency of velocity resonance. The frequency of oscillation varied from 2.46 to 6.24 hertz. The reduced-frequency parameter,  $\frac{\omega d}{2V}$ , varied from 0.0114 to 0.1319 in pitch and from 0.0066 to 0.0528 in yaw.

The tests in pitch were made with the lower flaps inadvertently reversed; i.e., the left flap was installed on the right side and vice versa. The bottom photograph of figure 3 shows the lower flaps as installed in the reversed locations. It is believed that the effect of this reversal was negligible on the dynamic-stability characteristics.

#### DATA CORRECTIONS AND PRECISION

Tunnel-wall and model-support interference effects were assumed to be negligible and no corrections for these effects were made to the data. A  $0.2^\circ$  downflow in the test section at the centerline was taken into account in computing angle of attack.

For the data presented herein, values of the probable error of the various quantities are as follows:

	<u>Probable error</u>
Mach number, M .....	$\pm 0.002$
Mean angle of attack, $\alpha$ , deg .....	$\pm 0.1$
Reynolds number, R .....	$\pm 0.01 \times 10^6$
Damping-in-pitch parameter, $C_{m_q} + C_{m_{\dot{\alpha}}}$ , per radian .....	$\pm 0.2$
Oscillatory-longitudinal-stability parameter, $C_{m_{\alpha}} - k^2 C_{m_q}$ , per radian .....	$\pm 0.01$

Damping-in-yaw parameter,  $C_{n_r} - C_{n_\beta} \cos \alpha$ , per radian .....  $\pm 0.8$

Oscillatory-directional-stability parameter,  
 $C_{n_\beta} \cos \alpha + k^2 C_{n_r}$ , per radian .....  $\pm 0.02$

Reduced-frequency parameter,  $k$ , radians .....  $\pm 0.0003$

### TEST RESULTS

The results of these tests are presented graphically as follows:

Mach number, M	Longitudinal results, (a)	Lateral results
0.20	Fig. 5(a)	Fig. 6(a)
.40	(b)	(b)
.60	(c)	(c)
.80	(d)	(d)
.90	(e)	(e)
.95	(f)	(f)
1.00	(g)	(g)
1.20	(h)	(h)

<sup>a</sup>Lower flaps reversed. See section on test conditions.

Positive damping in pitch and positive oscillatory stability in pitch are indicated by negative values of  $C_{m_q} + C_{m_\alpha}$  and  $C_{m_\alpha} - k^2 C_{m_q}$ . Positive damping in yaw is indicated by negative values of  $C_{n_r} - C_{n_\beta} \cos \alpha$  while positive oscillatory stability in yaw is indicated by positive values of  $C_{n_\beta} \cos \alpha + k^2 C_{n_r}$ .

### Longitudinal Results

As can be seen from the data presented in figure 5, the damping in pitch

characteristics of the model are very dependent on flap position. With the flaps undeflected (configuration 1000) the damping in pitch is generally near zero or slightly positive and, except at the lower Mach numbers, shows considerable nonlinearity with angle of attack. With the flaps deflected (configuration 1320) the level of damping is generally increased and results in positive damping in pitch at all test conditions. In addition, the deflection of the flaps eliminates most of the nonlinearity in the damping characteristics with angle of attack.

The configuration with the flaps undeflected (configuration 1000) has large regions of negative stability except at the lower Mach numbers. As is the damping parameter, the stability parameter for this configuration is very nonlinear with angle of attack.

The flaps have a very strong effect on the oscillatory-longitudinal stability parameter. In general the configuration with the flaps deflected (configuration 1320) has positive stability throughout the angle of attack range except for the higher angles of attack.

#### Lateral Results

The damping-in-yaw characteristics presented in figure 6 indicate that both configurations have positive damping in yaw at all test conditions. As with the pitch characteristics, the configuration with the flaps undeflected (configuration 1000) exhibits considerable nonlinearity in its yaw characteristics with angle of attack except for the lower Mach numbers. Except at the higher angles of attack at near-sonic speeds, the configuration with the flaps deflected (configuration 1320) has a fairly linear variation in yaw damping

with angle of attack. For both configurations there is generally a slight increase in yaw damping with increasing angle of attack.

Both configurations generally exhibit a decrease in stability in yaw with angle of attack as might be expected due to the tail surfaces being submerged in the wake of the body. The configuration with the flaps deflected (configuration 1320) has positive stability for angles of attack less than about  $12^\circ$  at all Mach numbers. However, except at the lower Mach numbers the configuration with the flaps undeflected (configuration 1000) is unstable over a large range of angle of attack. The regions of instability are especially large at Mach numbers from 0.60 to 0.90 and include the angles of attack near zero at Mach numbers of 0.90 and 0.95.

#### CONCLUDING REMARKS

Wind-tunnel measurements have been made of the aerodynamic damping and oscillatory stability characteristics in pitch and yaw for a sub-scale model of a proposed manned lifting entry vehicle at Mach numbers from 0.20 to 1.20. The measurements were made at angles of attack from  $-2^\circ$  to about  $22^\circ$  at  $0^\circ$  angle of sideslip by using a small-amplitude forced-oscillation technique. Models were tested with upper and lower control flaps both deflected and undeflected.

With undeflected flaps, the damping in pitch is generally near zero or slightly positive and, except at the lower Mach numbers, is nonlinear with angle of attack. With deflected flaps the level of damping is generally increased and results in positive damping in pitch at all test conditions. With undeflected flaps, the model exhibits negative stability in pitch except at the lower Mach numbers. In general, with flaps deflected the model has positive

stability throughout the angle of attack range except for the higher angles of attack.

Both configurations have positive damping in yaw which generally increases with increasing angle of attack. Both configurations generally exhibit a decrease in stability in yaw with angle of attack. The configuration with flaps deflected has positive stability for angles of attack less than about  $12^{\circ}$ . However, except at the lower Mach numbers the configuration with flaps undeflected is unstable over a large range of angle of attack.

## REFERENCES

1. Kilgore, Robert A, and Davenport, Edwin E. : Aerodynamic Damping and Oscillatory Stability in Pitch of a Model of a Proposed Manned Lifting Entry Vehicle at Mach Numbers of 1.80, 2.16, and 2.86. NASA TM X-72636, 1975.
2. Mechtly, E. A. : The International System of Units - Physical Constants and Conversion Factors - Second Revision. NASA SP-7012, 1973.
3. Schaefer, William T., Jr. : Characteristics of Major Active Wind Tunnels at the Langley Research Center. NASA TM X-1130, 1965.
4. Wright, Bruce R., and Kilgore, Robert A. : Aerodynamic Damping and Oscillatory Stability in Pitch and Yaw of Gemini Configurations at Mach Numbers from 0.50 to 4.63. NASA TN D-3334, 1966.

TABLE I  
GEOMETRIC CHARACTERISTICS OF MODEL

Reference area, $A$ , $m^2$	0.0963
Reference length, $d$ , $m$	
Pitch	0.5608
Yaw	0.2438
Body (without fins), $B^{20}$	
Length, $m$	0.5725
Plan area, $m^2$	0.0956
Width, $m$	0.2438
Height, $m$	0.1341
Center fin, $F^{64}$	
Airfoil section	Slab
Area, $m^2$	0.00927
Aspect ratio	0.54
Leading edge sweep	$55^\circ$
Root chord, $m$	0.1753
Tip chord, $m$	0.0875
Taper ratio	0.499
Span, $m$	0.0707
Thickness, $m$	0.0101
Tip fins, $F^{65}$	
Airfoil	Cambered with leading edge droop
Area (true, per fin), $m^2$	0.01477
Aspect ratio	0.61

TABLE I.- Concluded

Dihedral (angle with respect to vertical)		16°
Incidence (leading edge toed in)		4°
Leading edge sweep (projected side view)		55°
Root chord, m		0.2070
Tip chord, m		0.0930
Taper ratio		0.447
Span (root chord to tip chord), m		0.0948
Overall vehicle width (trailing edge tip between fins, theoretical), m		0.3252
Rudder, R <sup>64</sup>		
Area, m <sup>2</sup>		0.00297
Hingeline sweep		9.78°
Rudder, R <sup>65</sup>		
Area, m <sup>2</sup>		0.00440
Hingeline sweep		9.78°
Flaps	Upper, T <sup>47</sup> and T <sup>48</sup>	Lower, T <sup>49</sup> and T <sup>50</sup>
Area, m <sup>2</sup>	0.00644	0.00832
Chord, m	.0692	.0914
Span, m	.1018	.1079
Hingeline sweep	0°	10.47°
Canopy, C <sup>10</sup>		
Length, m		0.1956
Width, m		0.0675
Windshield angle		55°

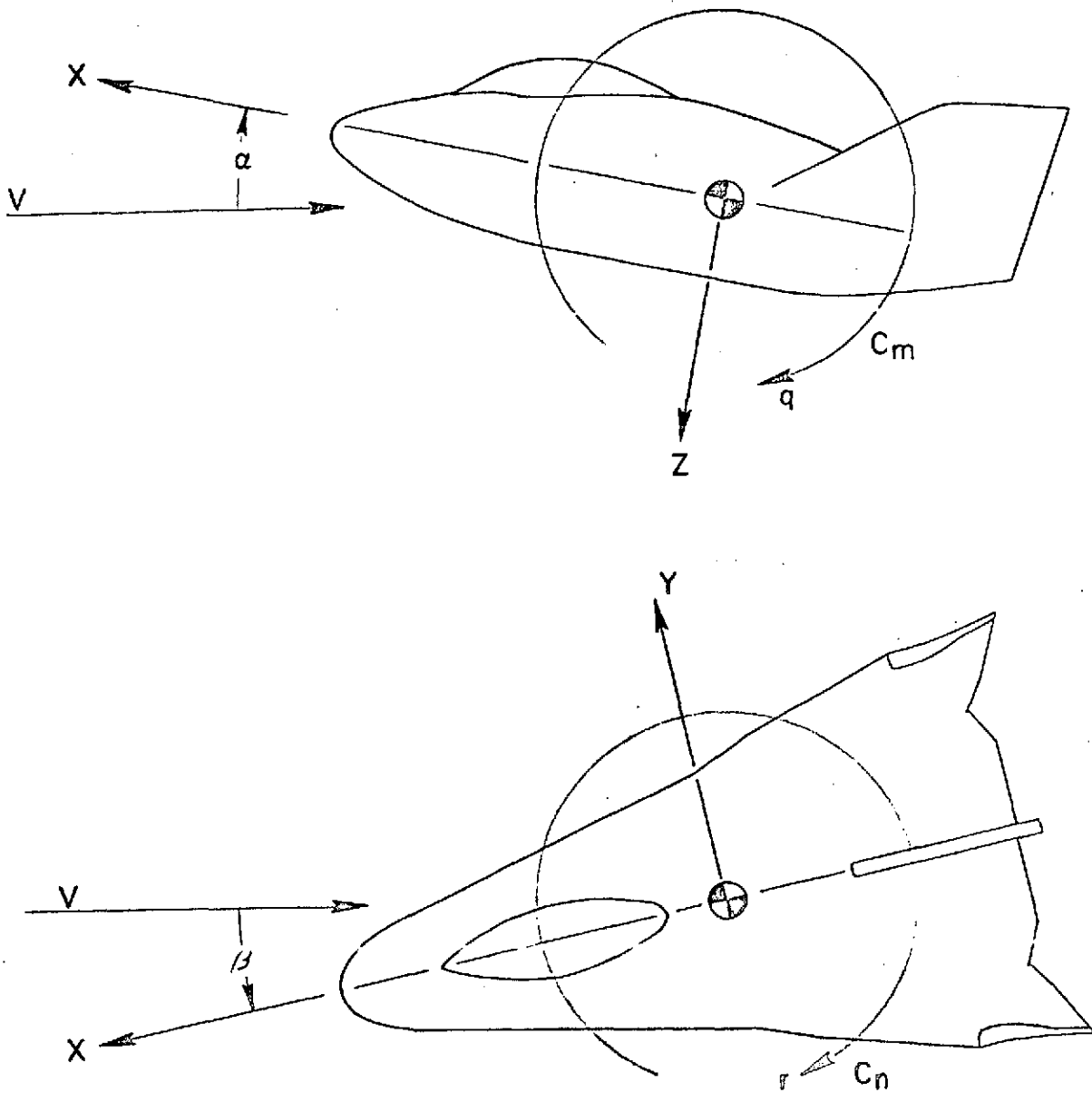


FIGURE 1.- Body system of axes. Coefficients, angles, and angular velocities shown in positive sense.

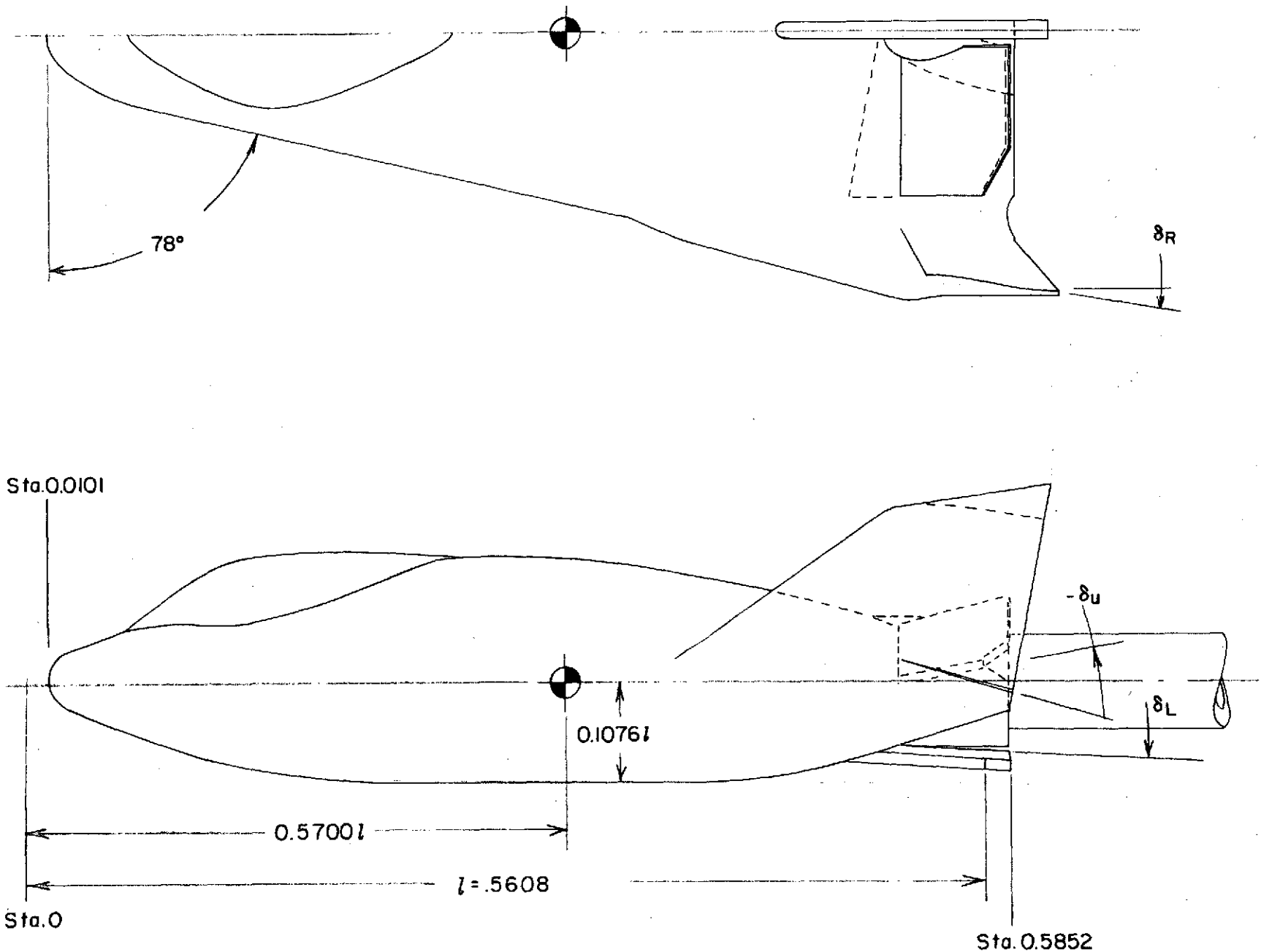
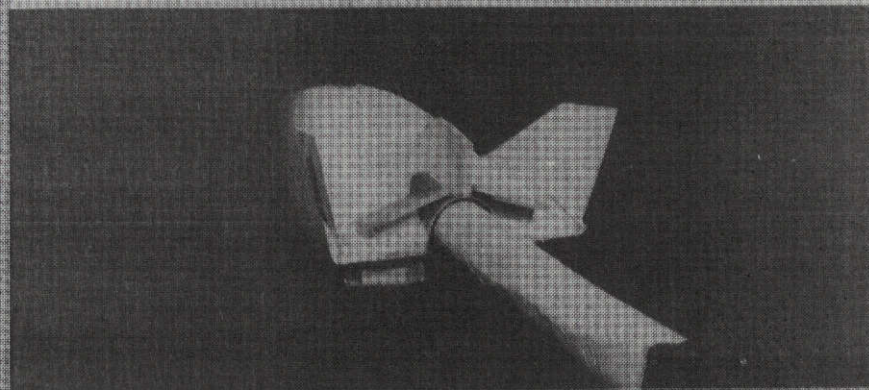
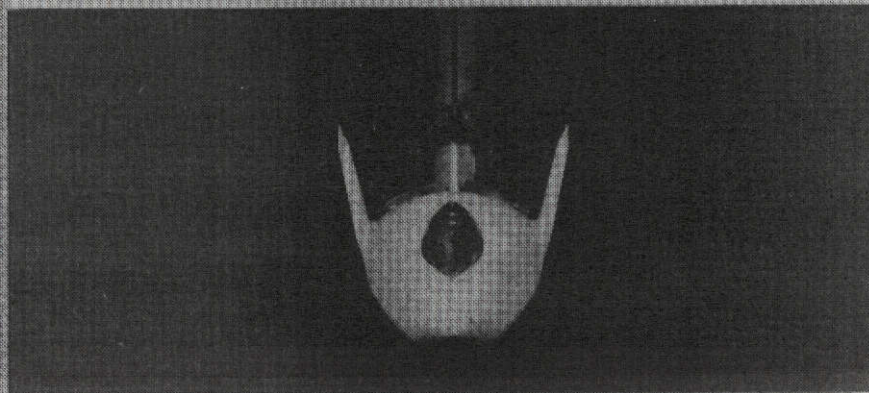
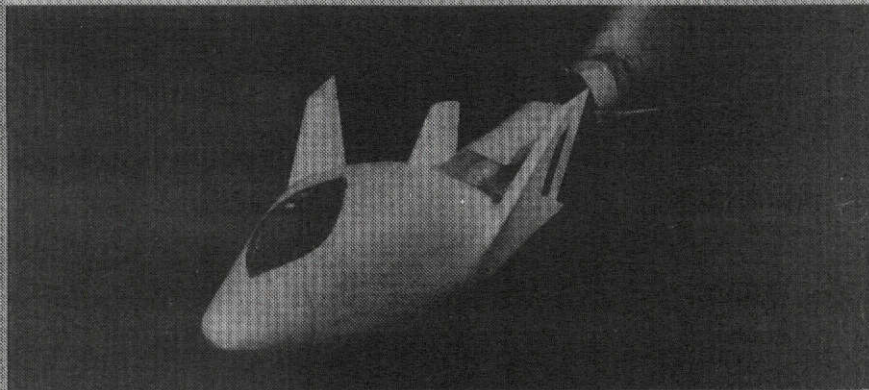


Figure 2. - Design dimensions of model of proposed aircraft.



*Figure 3. - Photographs of Configuration 1320 mounted on oscillation balance mechanism.*

*(Bottom photograph shows lower flaps reversed. See section on Test Conditions.)*

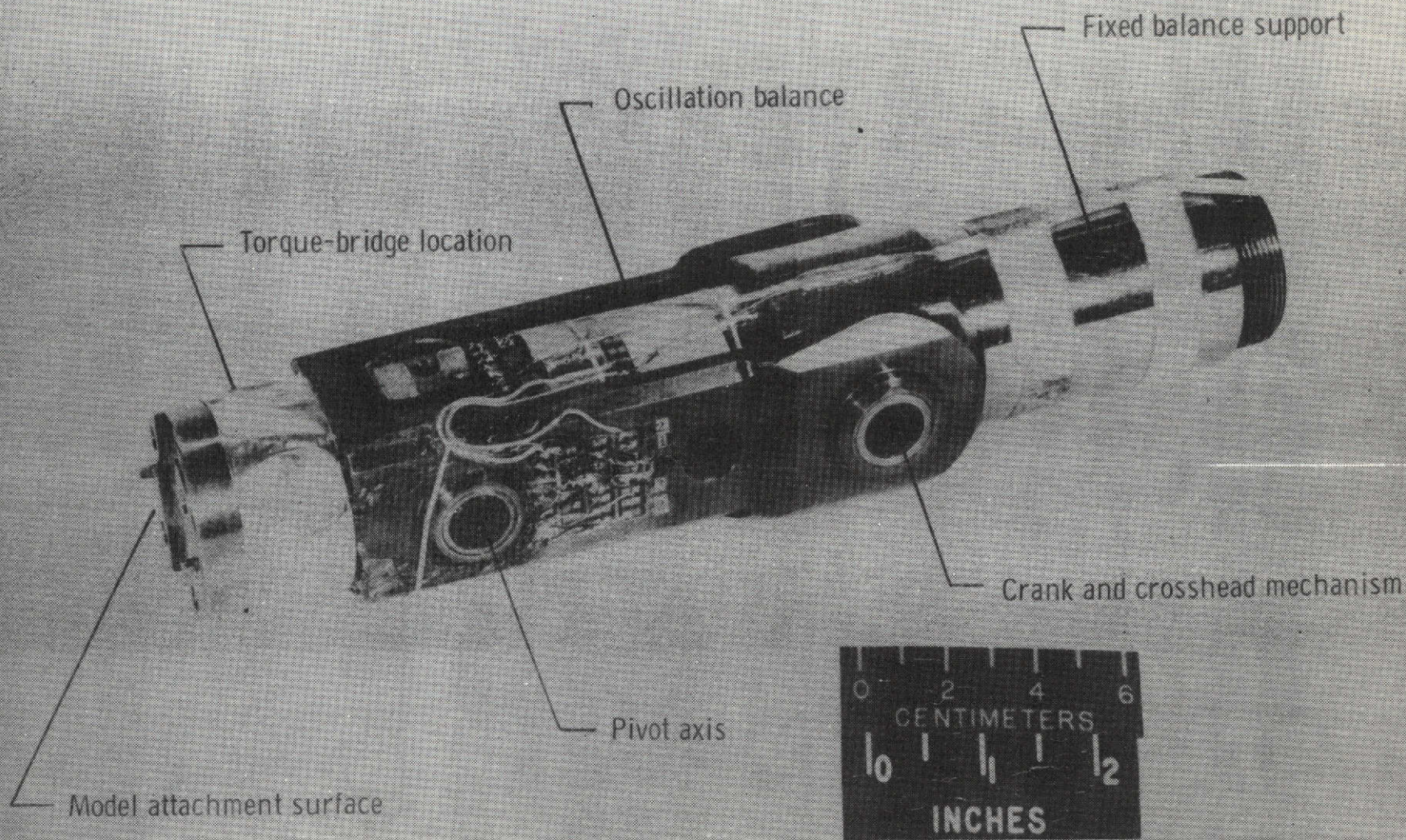
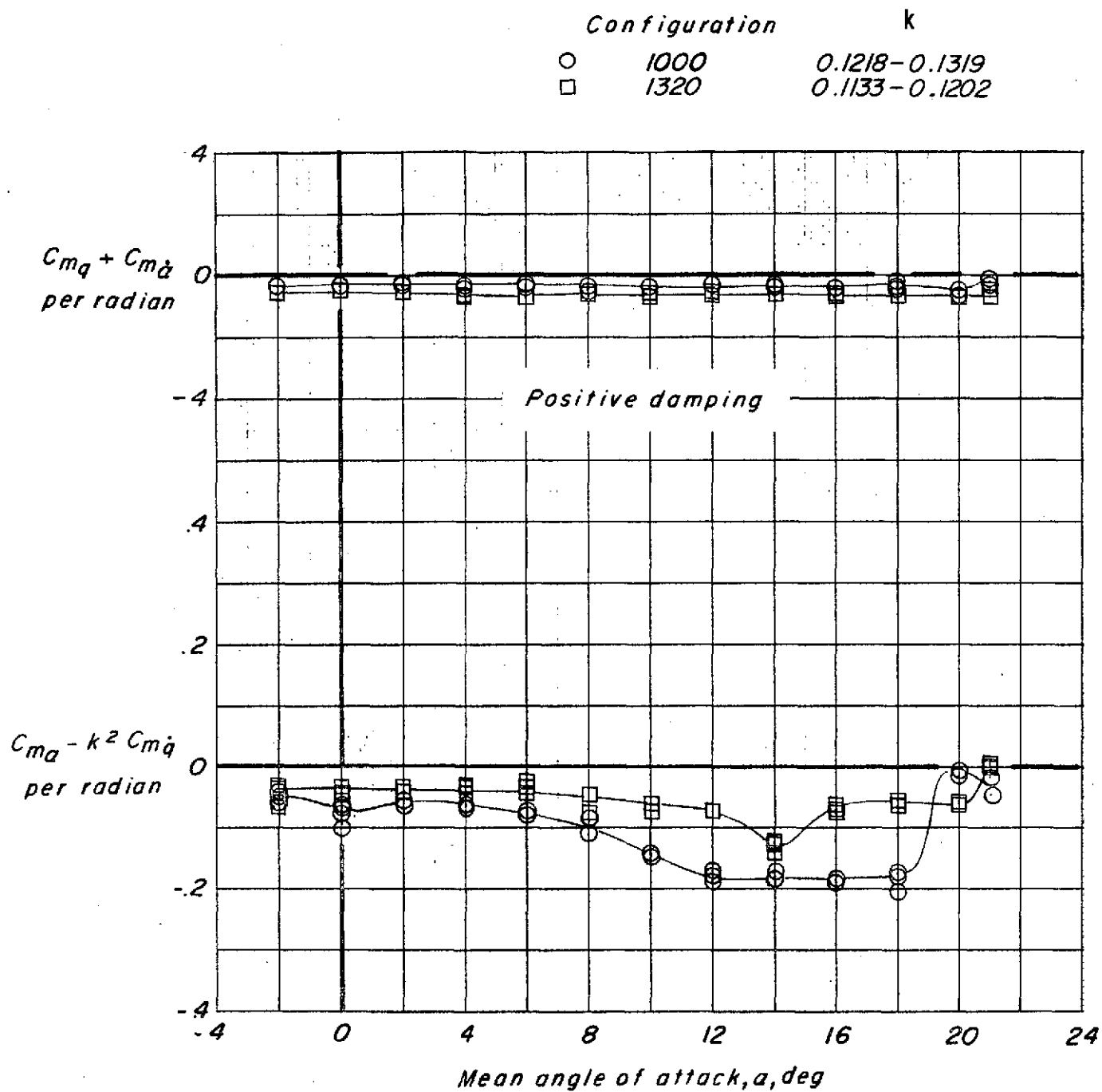


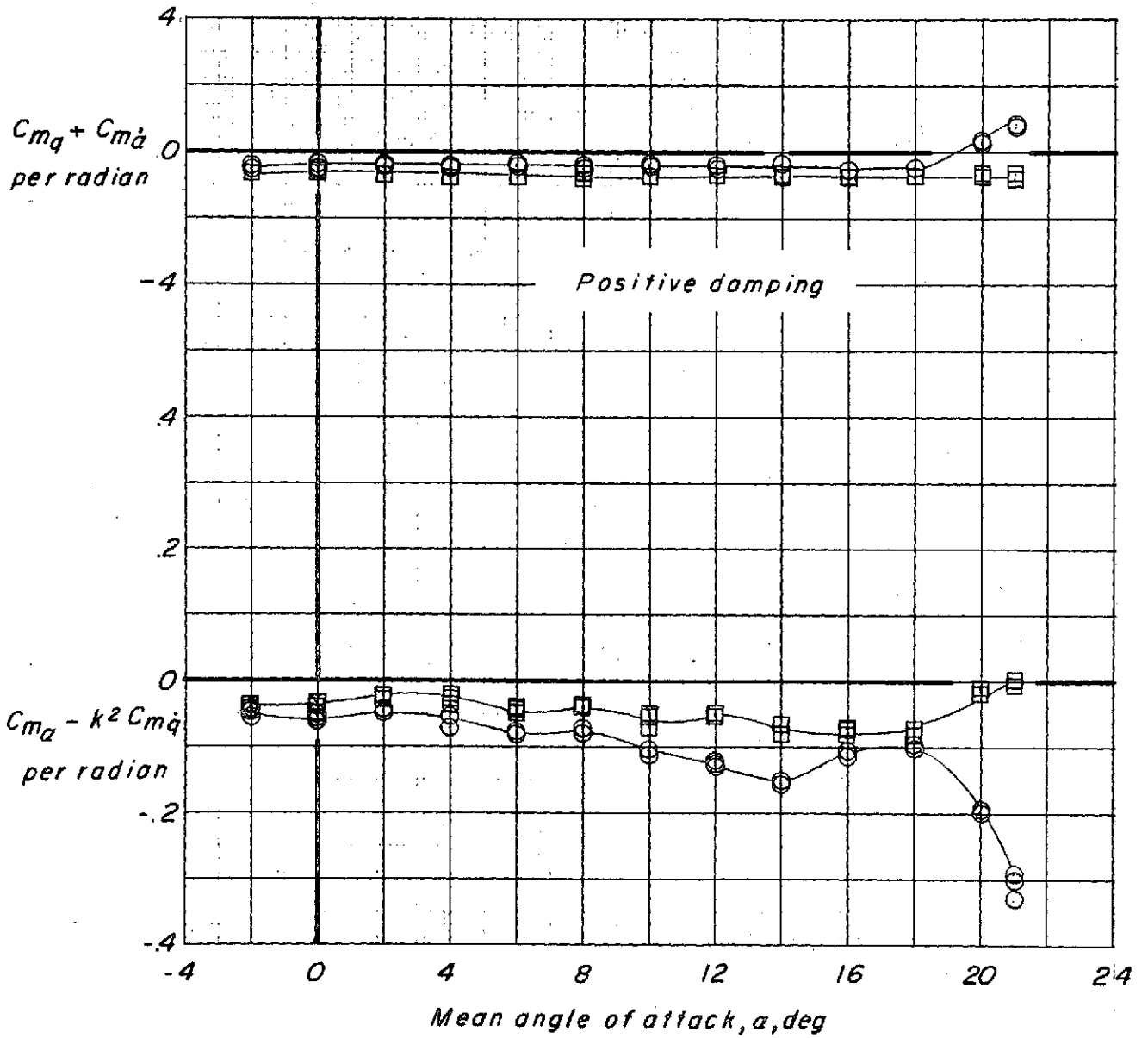
Figure 4.- Forward portion of oscillation-balance mechanism.



(a)  $M = 0.20$ ,  $R = 3.35 \times 10^6$

Figure 5.- Variation of damping-in-pitch parameter and oscillatory-longitudinal stability parameter with mean angle of attack for configurations 1000 and 1320 at subsonic and transonic speeds. (Lower flaps reversed. See section on test conditions.)

Configuration	k
○ 1000	0.0635-0.0772
□ 1320	0.0573-0.0611



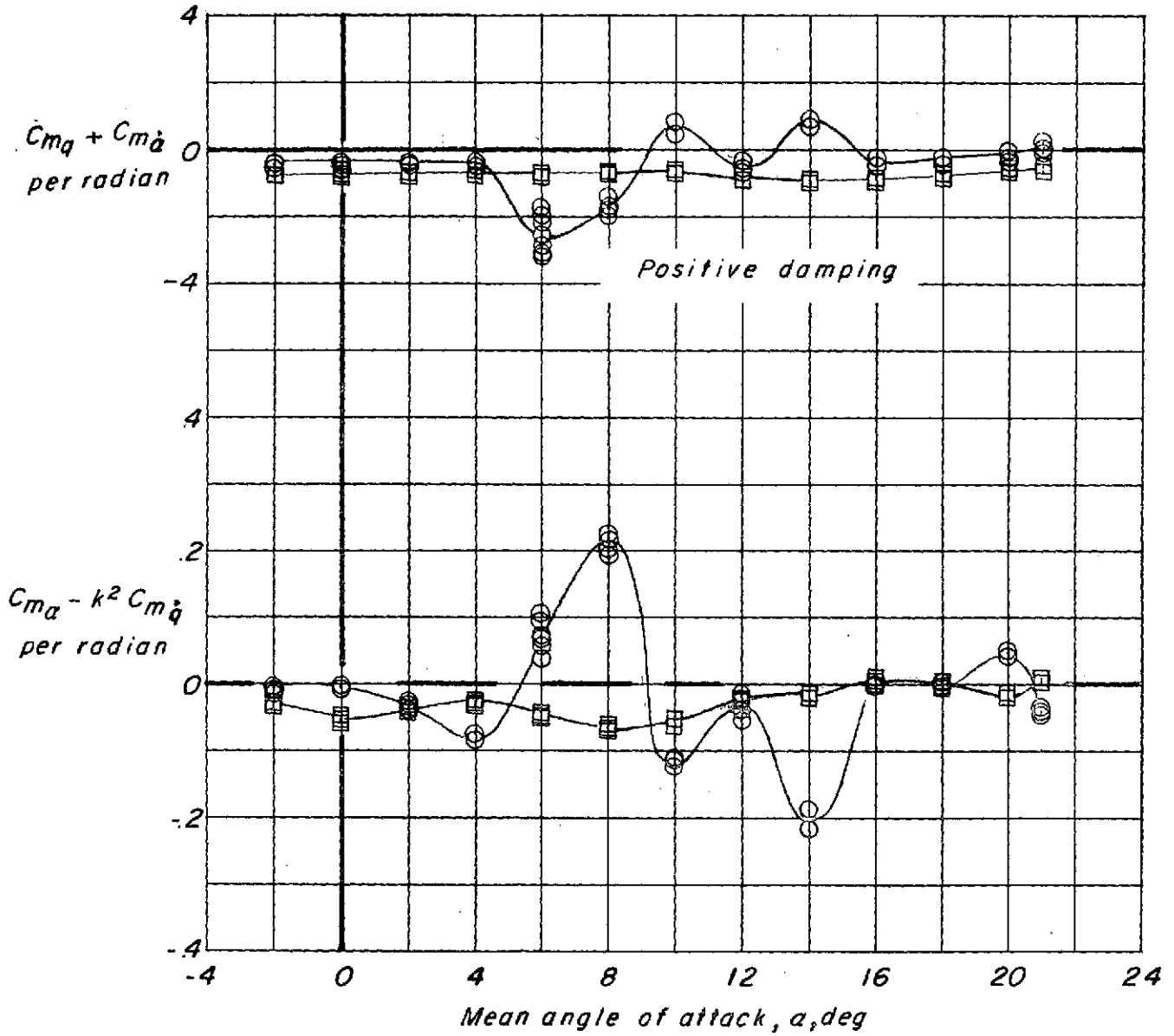
(b)  $M = 0.40$ ,  $R = 3.38 \times 10^6$

Figure 5. - Continued.

Configuration

k

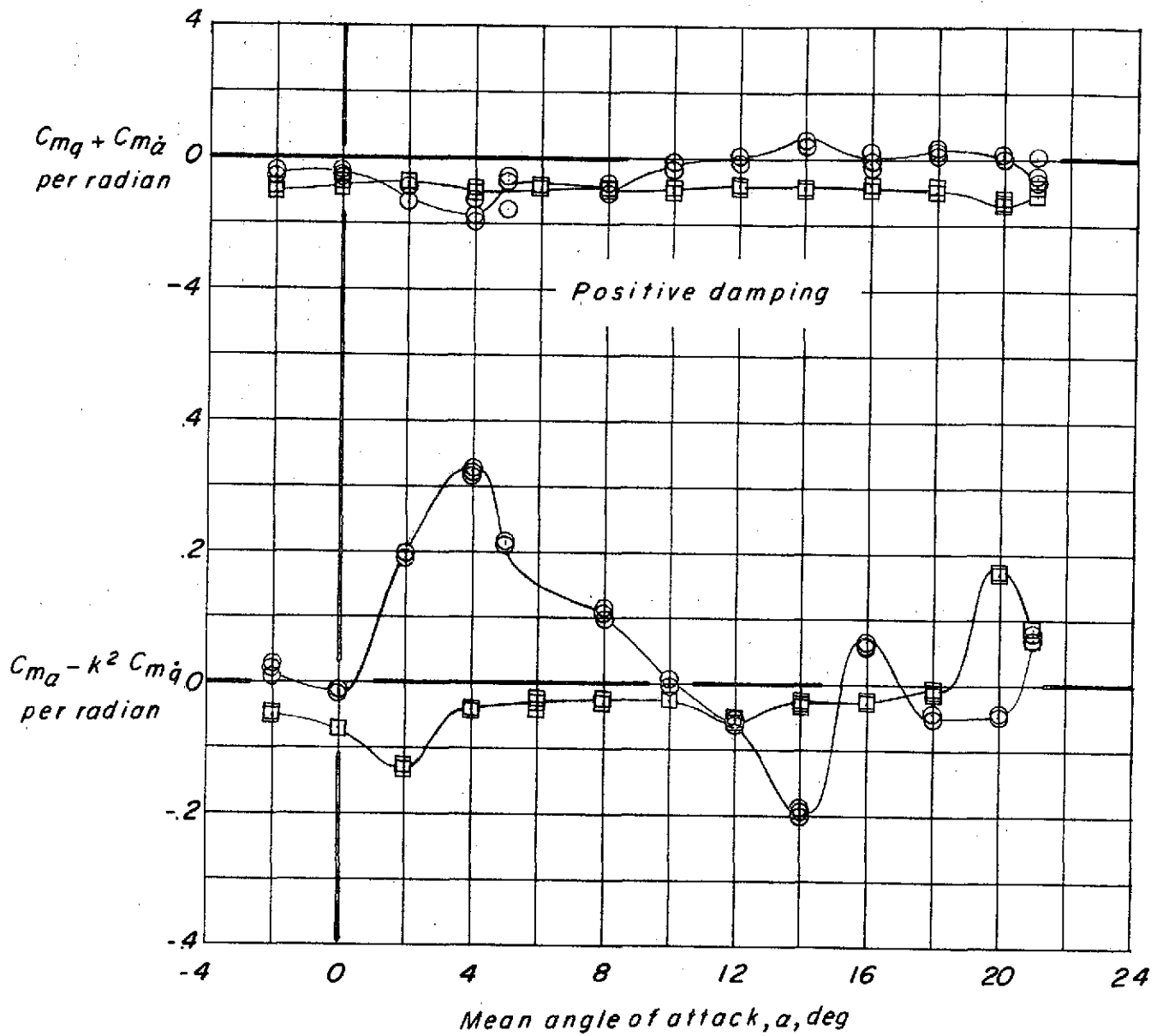
○	1000	0.0288-0.0523
□	1320	0.0379-0.0423



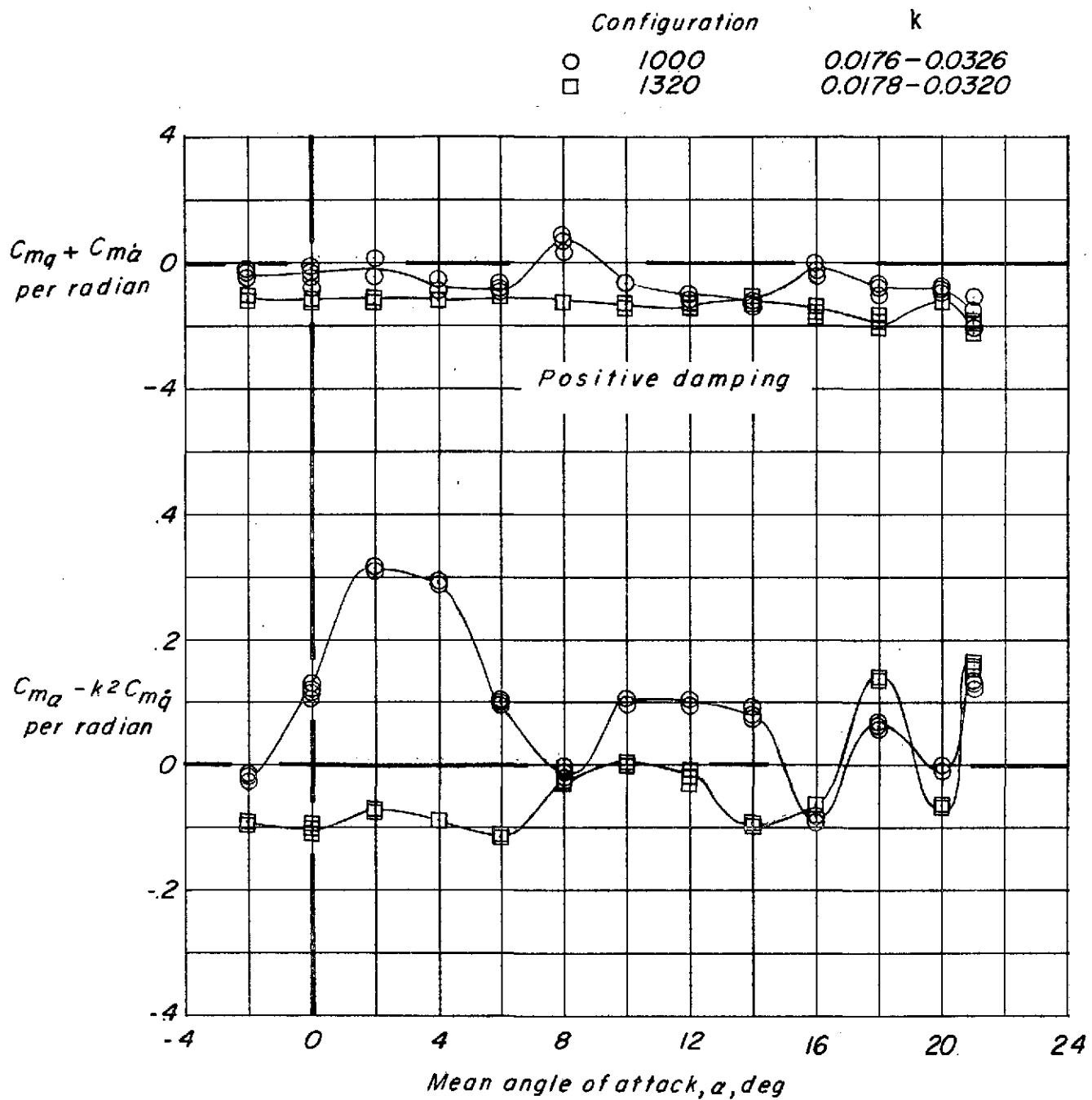
(c)  $M = 0.60$ ,  $R = 3.48 \times 10^6$

Figure 5. - Continued.

Configuration	k
○	1000 0.0187-0.0406
□	1320 0.0203-0.0358

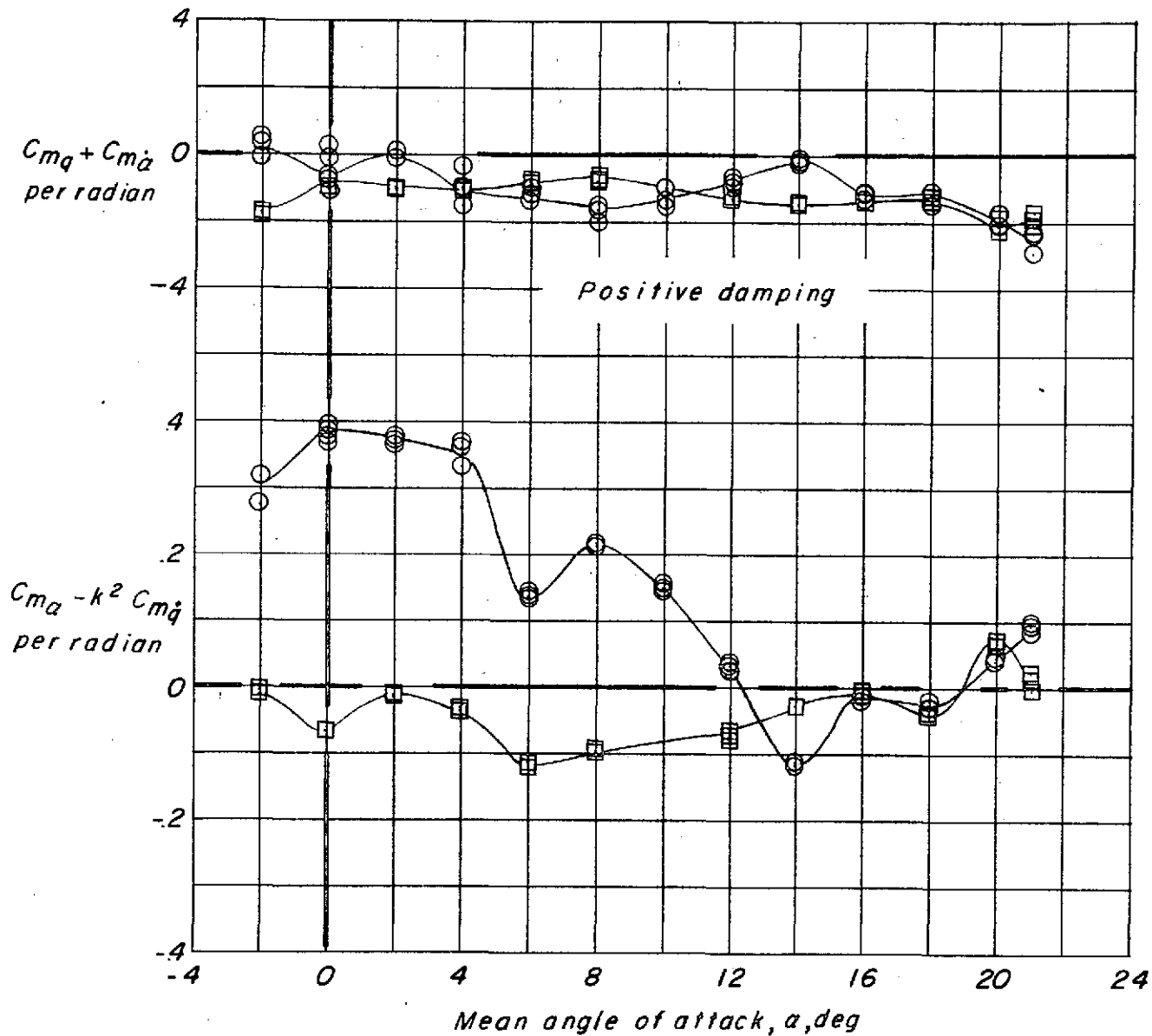


(d)  $M = 0.80, R = 3.46 \times 10^6$   
 Figure 5. - Continued.



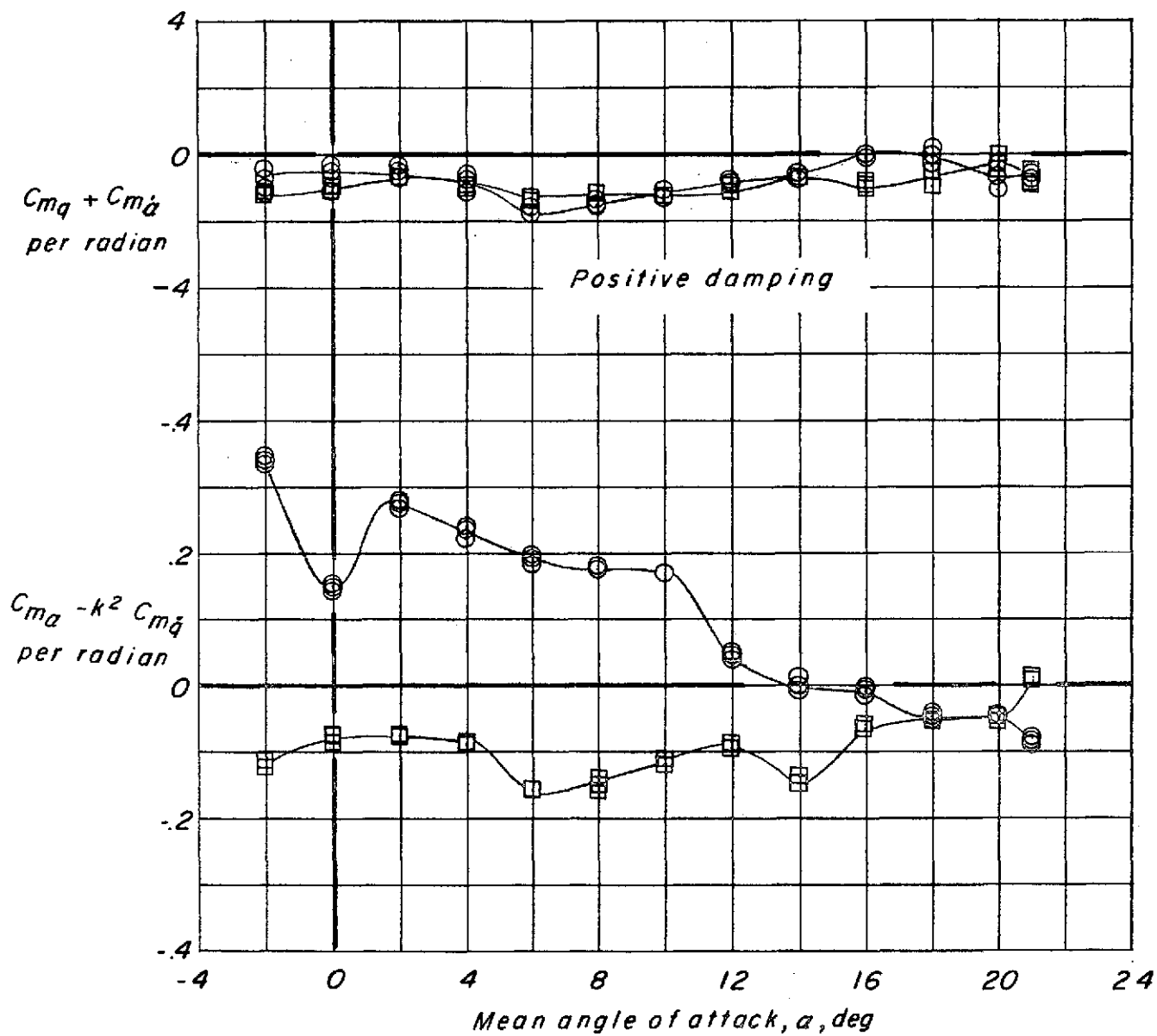
(e)  $M = 0.90$ ,  $R = 3.49 \times 10^6$   
 Figure 5. - Continued.

Configuration	k
○ 1000	0.0140-0.0330
□ 1320	0.0226-0.0306



(f)  $M = 0.95, R = 3.47 \times 10^6$   
 Figure 5. - Continued.

Configuration	k
○ 1000	0.0132-0.0305
□ 1320	0.0237-0.0309



(g)  $M = 1.00$ ,  $R = 3.43 \times 10^6$

Figure 5. - Continued.

Configuration

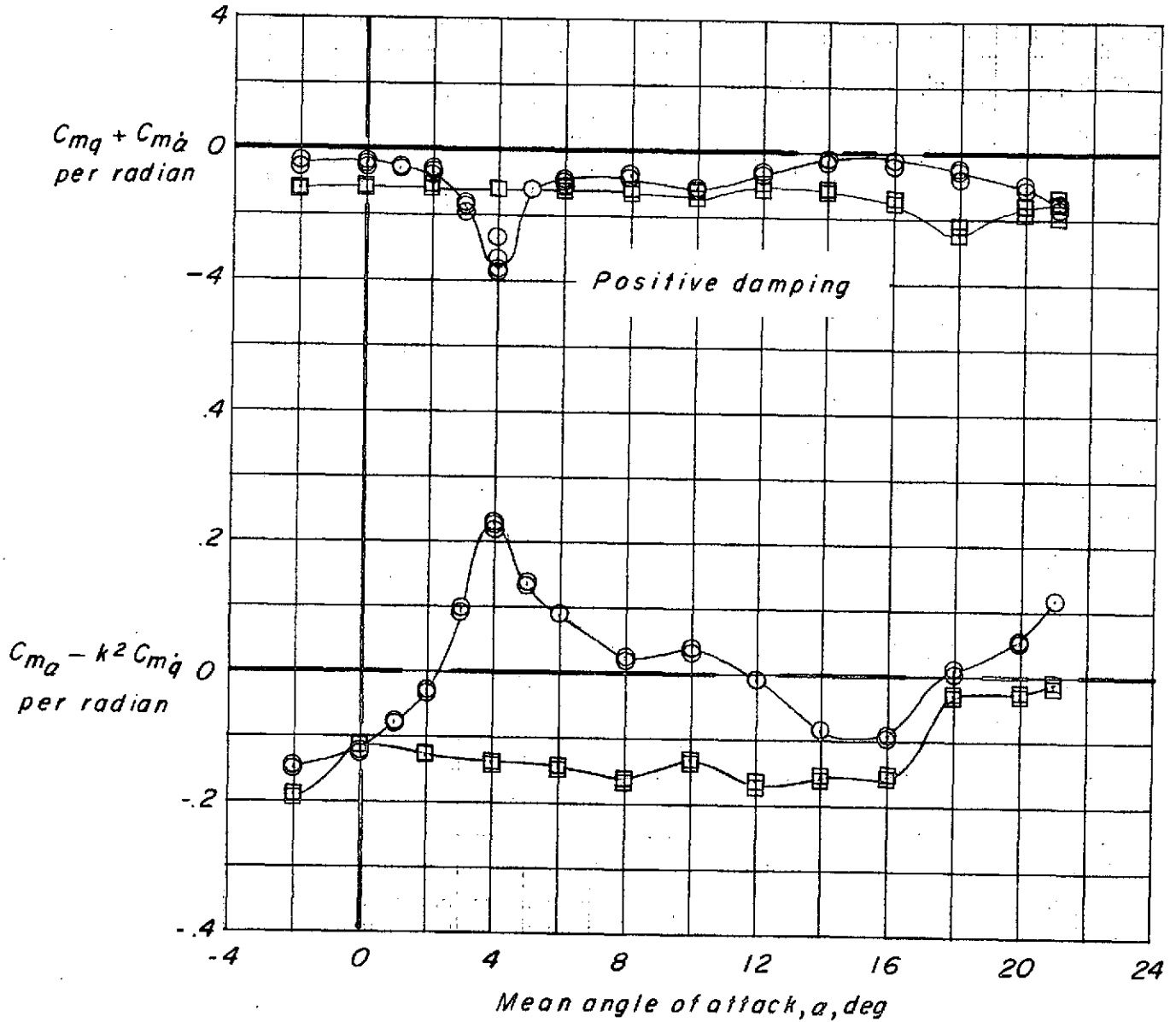
k

○ 1000

0.0115-0.0288

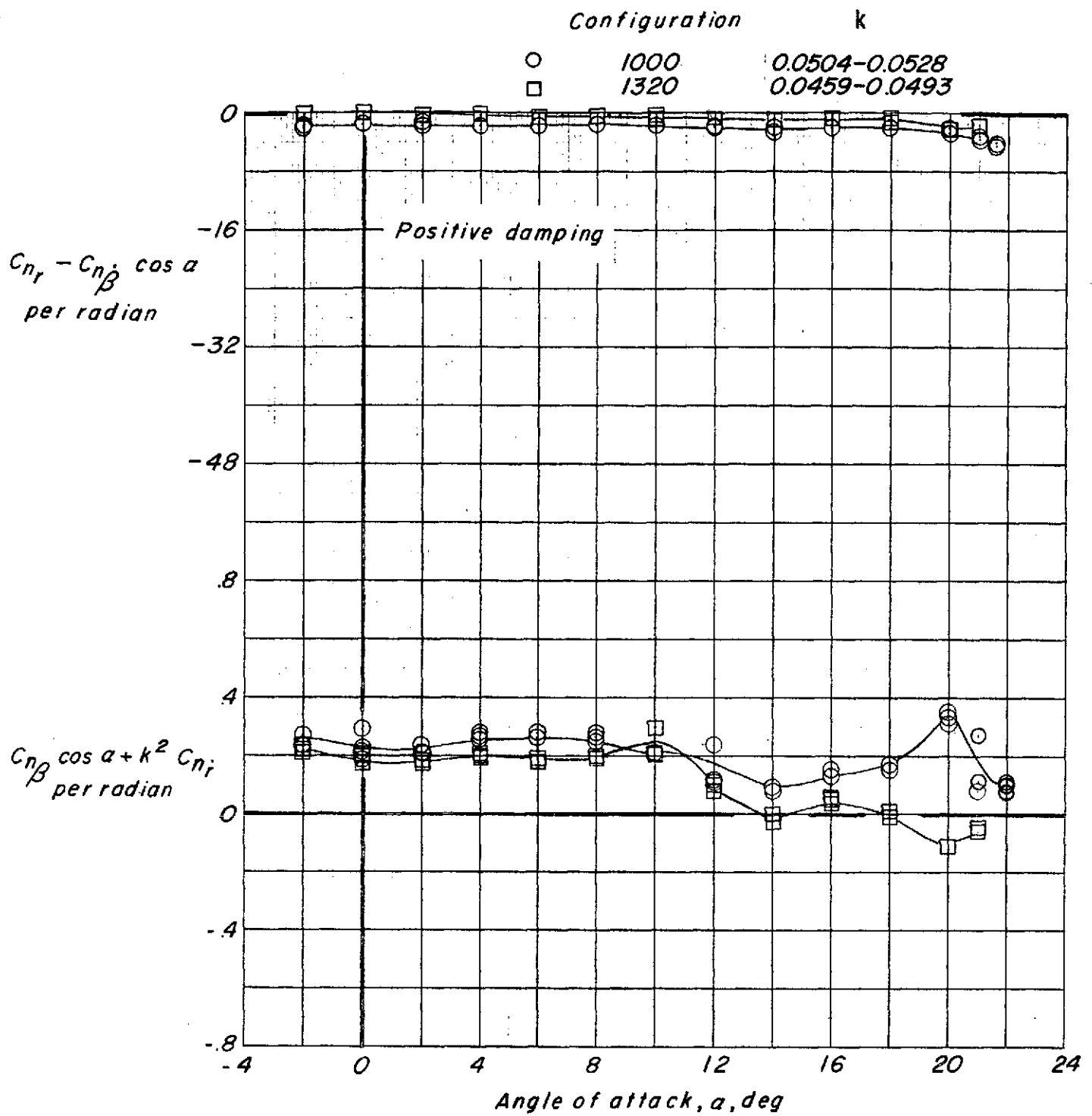
□ 1320

0.0219-0.0282



(h)  $M = 1.20$ ,  $R = 3.46 \times 10^6$

Figure 5. - Concluded.



(a)  $M = 0.20$ ,  $R = 3.35 \times 10^6$

Figure 6. - Variation of damping-in-yaw parameter and oscillatory directional stability parameter with angle of attack for configurations 1000 and 1320 at subsonic and transonic speeds.

Configuration

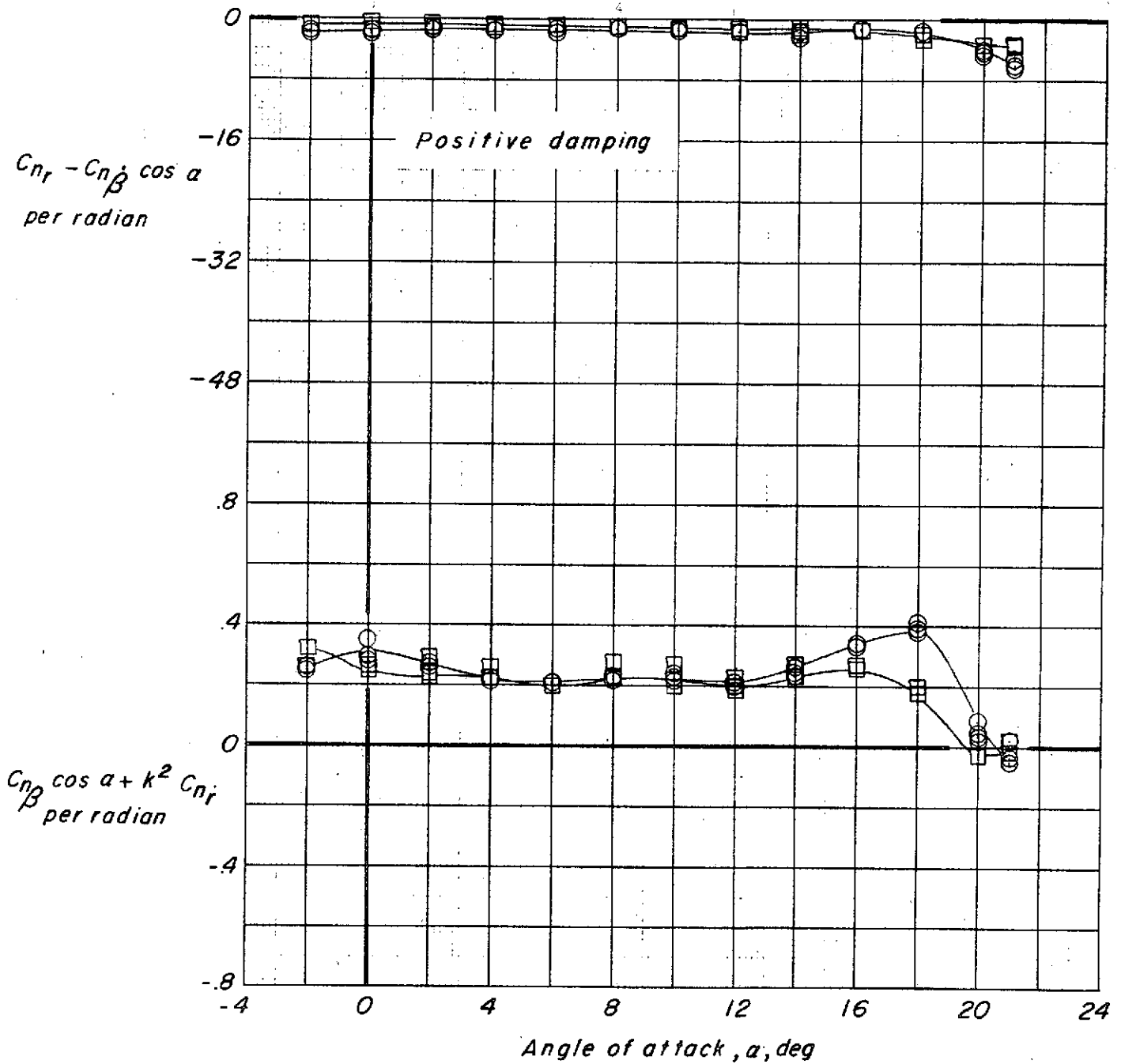
k

○ 1000

0.0244-0.0287

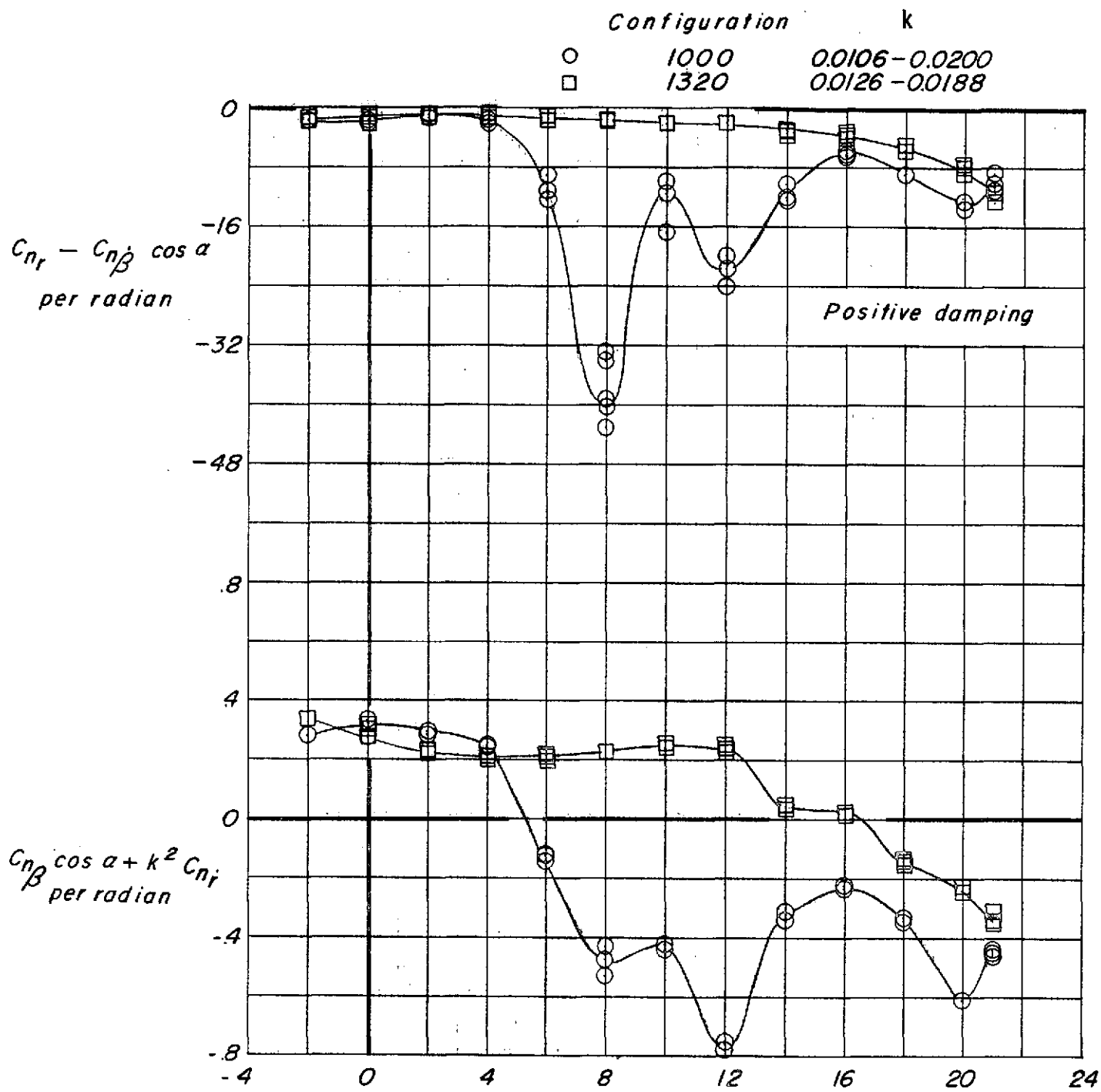
□ 1320

0.0237-0.0266



(b)  $M = 0.40$ ,  $R = 3.38 \times 10^6$

Figure 6. - Continued.

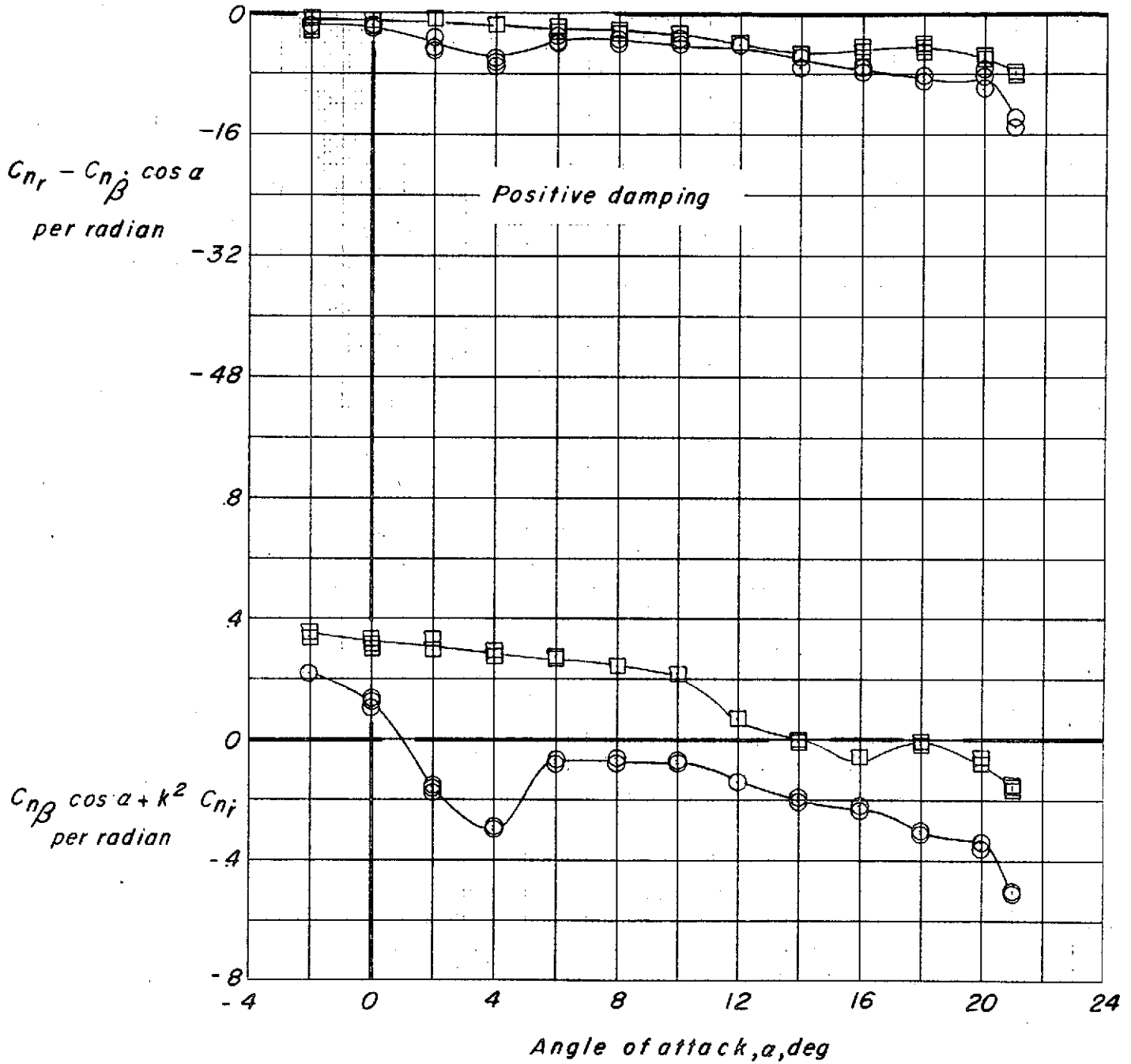


Angle of attack,  $\alpha$ , deg

(c)  $M = 0.60$ ,  $R = 3.48 \times 10^6$

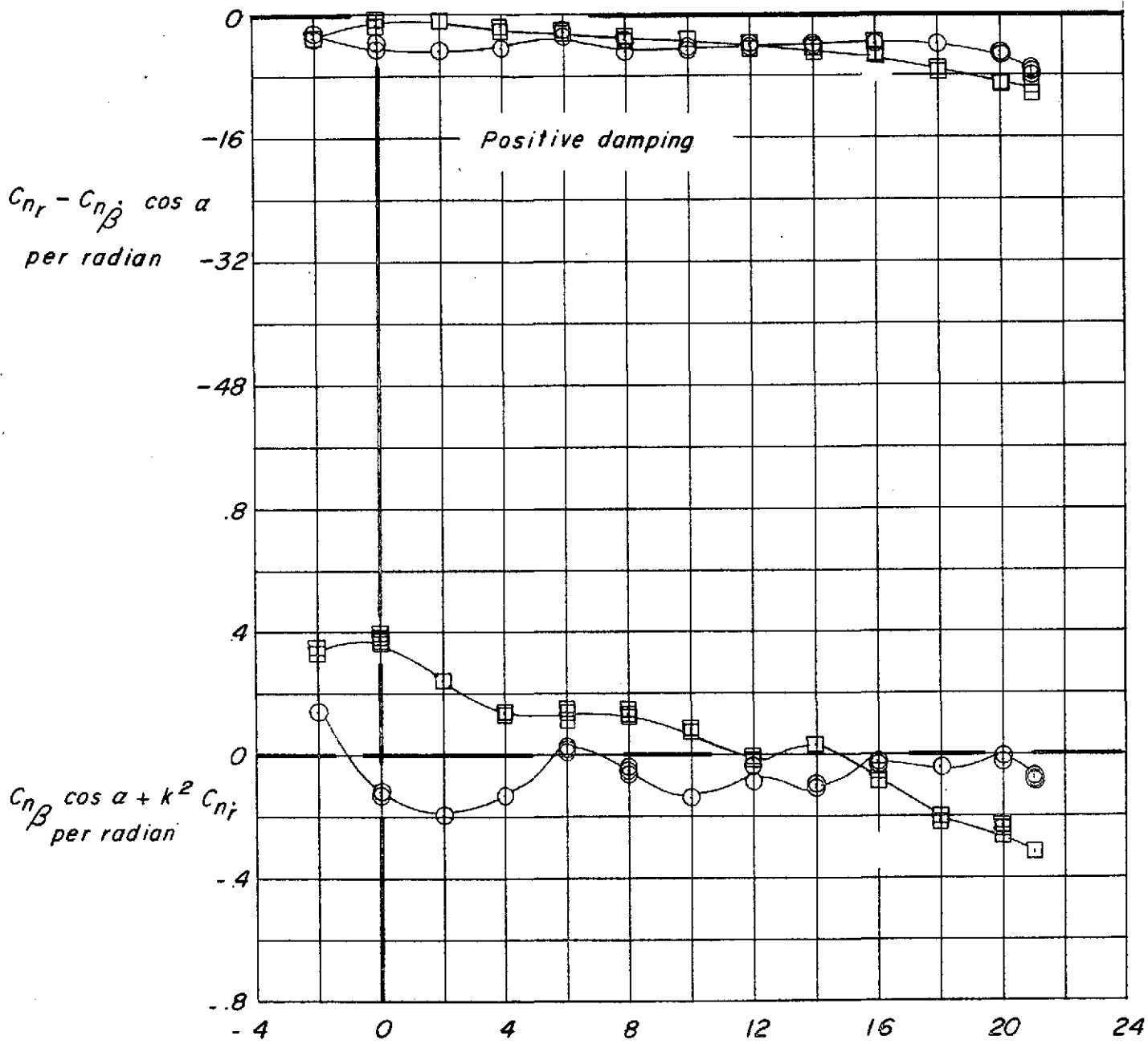
Figure 6. - Continued.

Configuration	k
○	1000 0.0072-0.0149
□	1320 0.0110-0.0152



(d)  $M = 0.80, R = 3.46 \times 10^6$   
 Figure 6. - Continued.

<i>Configuration</i>		<i>k</i>
○	1000	0.0099-0.0130
□	1320	0.0081-0.0140



Angle of attack,  $\alpha$ , deg

(e)  $M = 0.90$ ,  $R = 3.49 \times 10^6$

Figure 6. - Continued.

Configuration

k

○

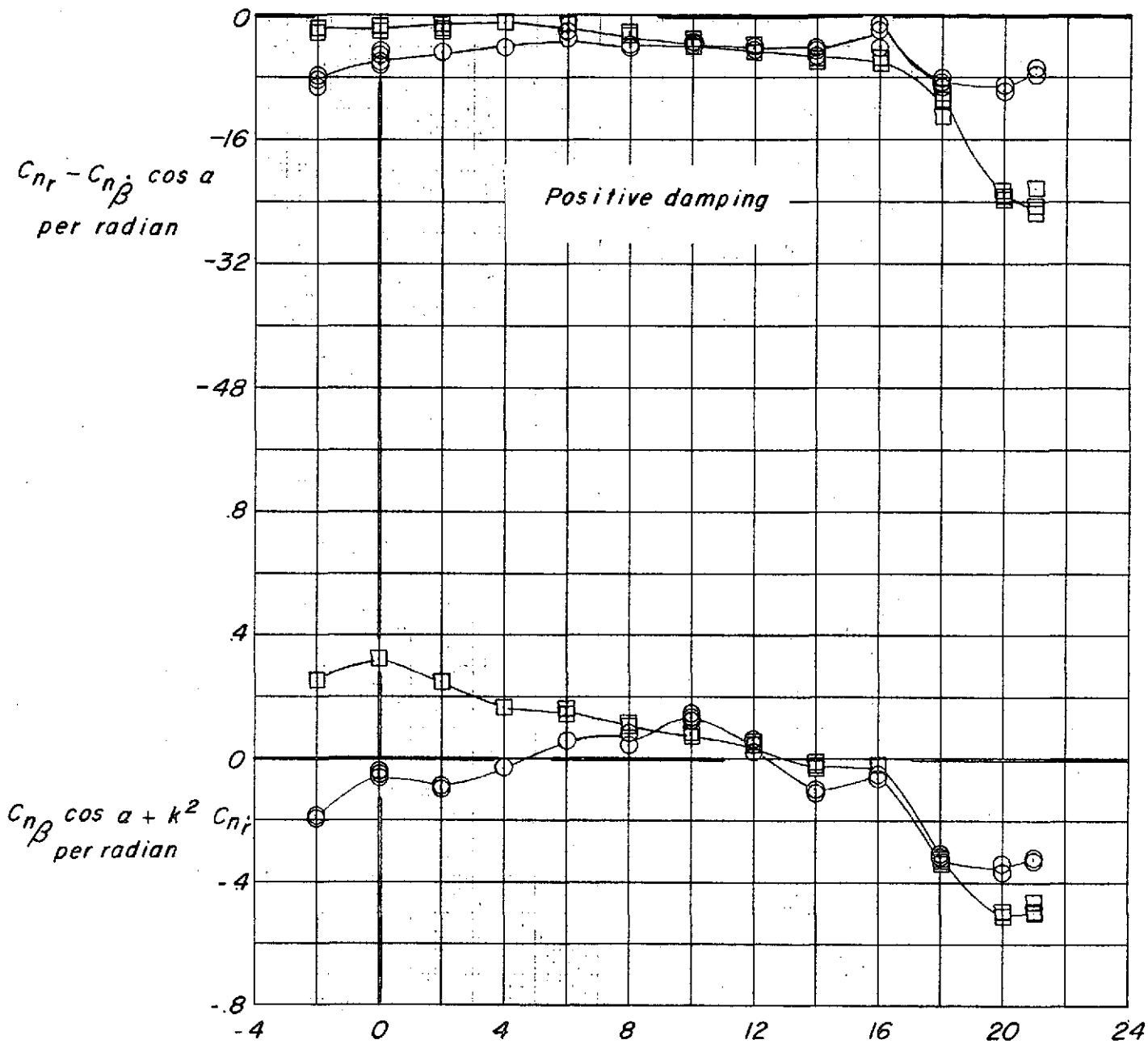
1000

0.0076-0.0124

□

1320

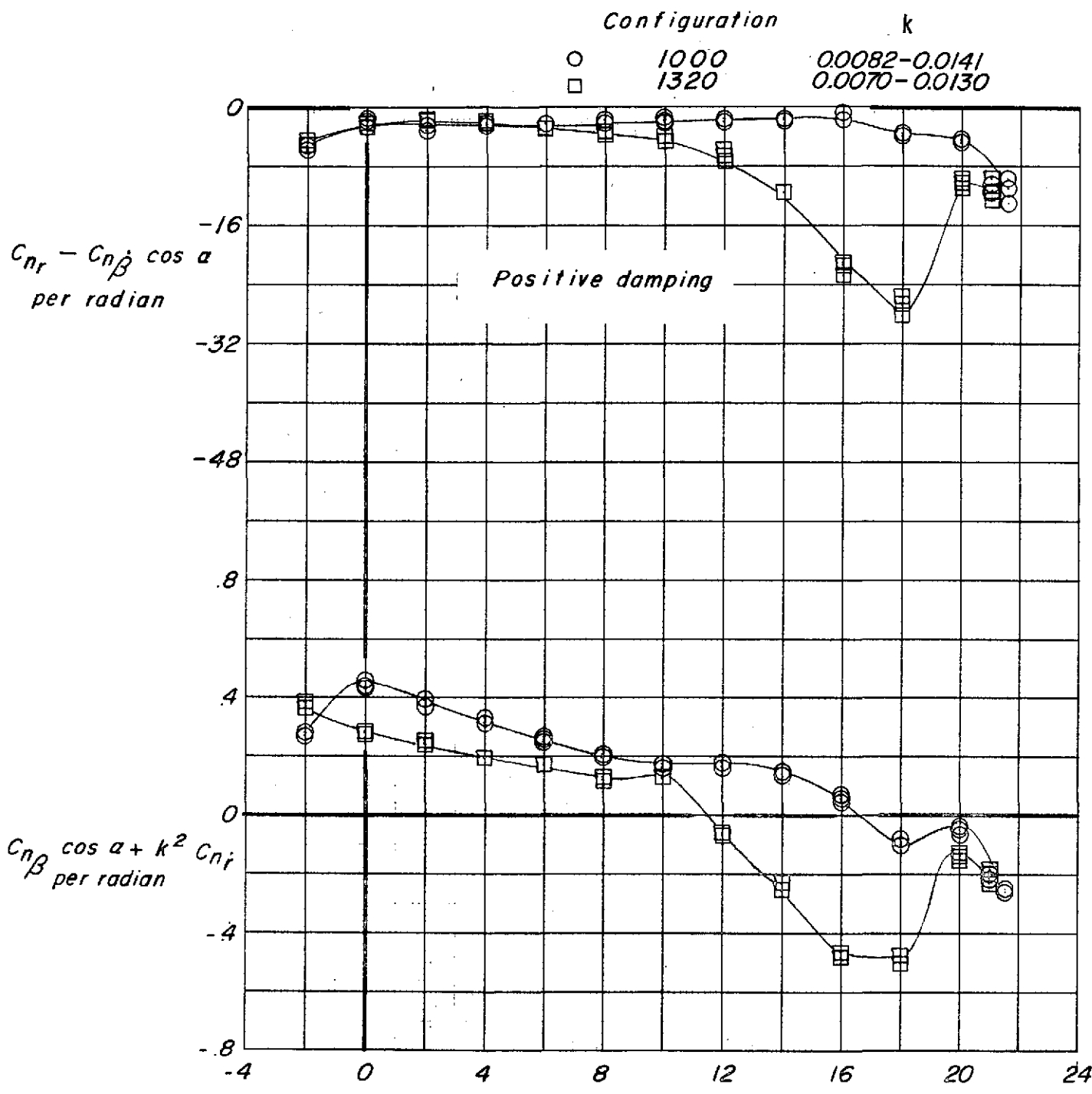
0.0073-0.0130



Angle of attack,  $\alpha$ , deg

(f)  $M = 0.95$ ,  $R = 3.47 \times 10^6$

Figure 6. - Continued.

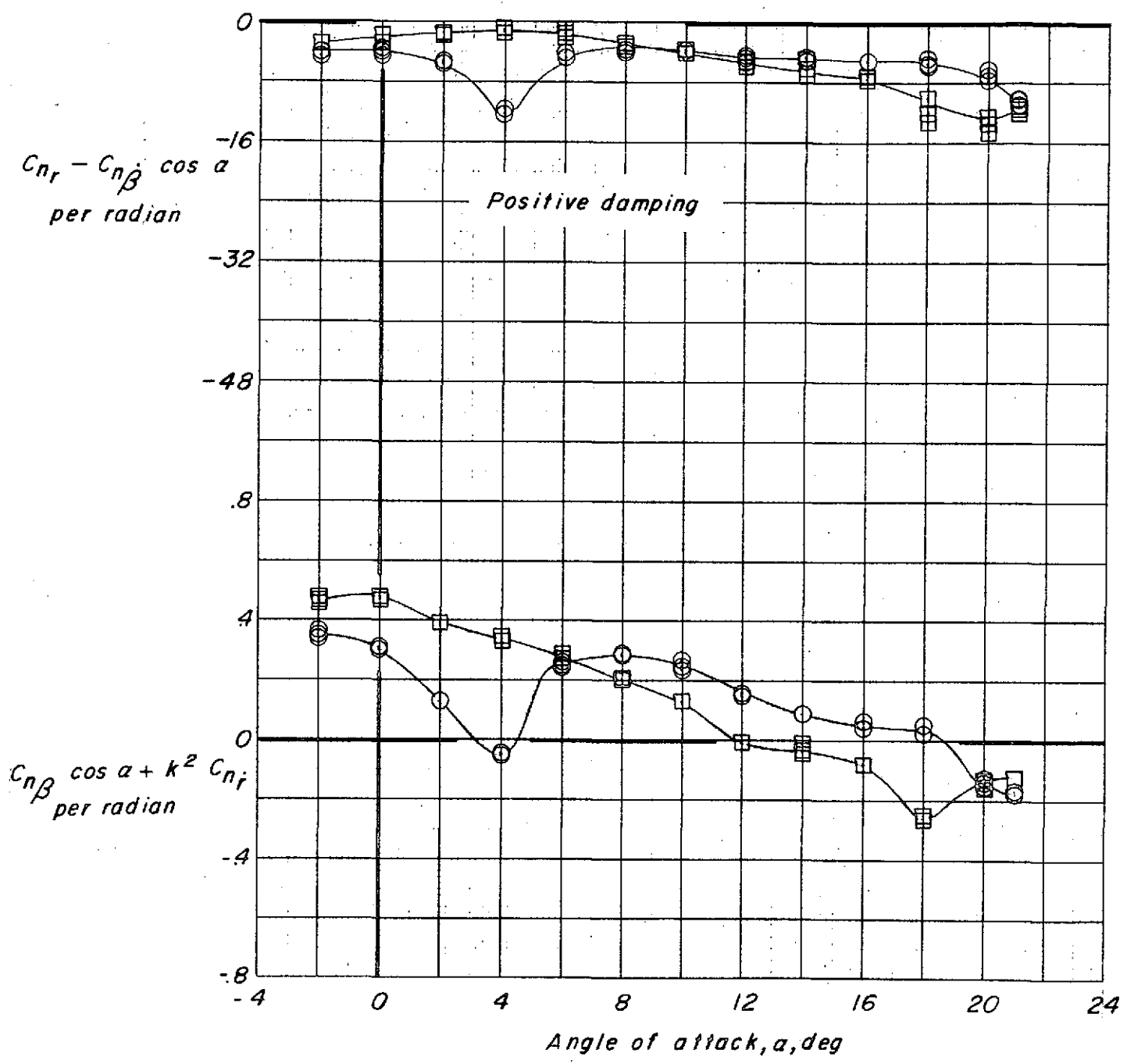


$C_{n_r} - C_{n\dot{\beta}} \cos \alpha$   
per radian

Positive damping

$C_{n\beta} \cos \alpha + k^2 C_{n_r}$   
per radian

Configuration	k	
○	1000	0.0078-0.0114
□	1320	0.0066-0.0119



(h)  $M = 1.20, R = 3.46 \times 10^6$   
 Figure 6. - Concluded.